Kaunas University of Technology

Faculty of Mechanical Engineering and Design

Development of a Wearable Assistance Rehabilitation Robot for Upper Limb

Master's Final Degree Project

Patrikas Tatariūnas

Project author

Prof. Egidijus Dragašius

Supervisor

Kaunas, 2023

Kaunas University of Technology

Faculty of Mechanical Engineering and Design

Development of a Wearable Assistance Rehabilitation Robot for Upper Limb

Master's Final Degree Project

Mechatronics (6211EX017)

Patrikas Tatariūnas

Project author

Prof. Egidijus Dragašius

Supervisor

Assoc. Prof. Rūta Rimašauskienė

Reviewer

Kaunas, 2023

Kaunas University of Technology

Faculty of Mechanical Engineering and Design

Patrikas Tatariūnas

Development of a Wearable Assistance Rehabilitation Robot for Upper Limb

Declaration of Academic Integrity

I confirm the following:

1. I have prepared the final degree project independently and honestly without any violations of the copyrights or other rights of others, following the provisions of the Law on Copyrights and Related Rights of the Republic of Lithuania, the Regulations on the Management and Transfer of Intellectual Property of Kaunas University of Technology (hereinafter – University) and the ethical requirements stipulated by the Code of Academic Ethics of the University;

2. All the data and research results provided in the final degree project are correct and obtained legally; none of the parts of this project are plagiarised from any printed or electronic sources; all the quotations and references provided in the text of the final degree project are indicated in the list of references;

3. I have not paid anyone any monetary funds for the final degree project or the parts thereof unless required by the law;

4. I understand that in the case of any discovery of the fact of dishonesty or violation of any rights of others, the academic penalties will be imposed on me under the procedure applied at the University; I will be expelled from the University and my final degree project can be submitted to the Office of the Ombudsperson for Academic Ethics and Procedures in the examination of a possible violation of academic ethics.

Patrikas Tatariūnas

Confirmed electronically

Kaunas University of Technology

Faculty of Mechanical Engineering and Design

Task of the Master's Final Degree Project

Given to the student – Patrikas Tatariūnas

1. Title of the Project

Development of a Wearable Assistance Rehabilitation Robot for Upper Limb

(In English)

Dėvimo pagalbinio roboto skirto rankos reabilitacijai kūrimas

(In Lithuanian)

2. Aim and Tasks of the Project

Aim: to develop a wearable assistance rehabilitation robot for patients with upper limb disability.
Tasks:

1. to analyse different types and control methods of existing assistance robots for upper limb rehabilitation;
2. to design the frame for wearable assistance rehabilitation robot and perform stress analysis;
3. to integrate applicable electronic components for control of the wearable assistance rehabilitation robot;
4. to perform a research on mechanical properties of 3D printed specimens from PLA for the wearable assistance rehabilitation robot frame;
5. to evaluate social, environmental and economical aspects of wearable assistance rehabilitation robot;

3. Main Requirements and Conditions

Autodesk Inventor, PLA plastic, 3 point bending test ISO:178 for plastics – determination of flexural stress, minimum safety factory for stress simulations – 3.

4. Additional Requirements for the Project, Report and its Annexes

Not applicable

Project author	Patrikas Tatariūnas		2023 03 03
	(Name, Surname)	*(Signature)*	*(Date)*
Supervisor	Egidijus Dragašius		2023 03 03
	(Name, Surname)	*(Signature)*	*(Date)*
Head of study field programs	Regita Bendikienė		2023 03 03
	(Name, Surname)	*(Signature)*	*(Date)*

Patrikas Tatariūnas. Development of a Wearable Assistance Rehabilitation Robot for Upper Limb. Master's Final Degree Project, supervisor Prof. Egidijus Dragašius; Faculty of Mechanical Engineering and Design, Kaunas University of Technology.

Study field and area (study field group): Production and Manufacturing Engineering (E10), Engineering Sciences (E).

Keywords: upper limb rehabilitation; wearable assistance rehabilitation robot; PLA plastic; 3D printing FDM technology; ISO:178 3 point bending test.

Kaunas, 2023. 52 p.

Summary

Upper limb motoric function disorder can be caused by many things including sport injuries, accidents, health related problems or strokes. A person affected by this disability not only faces physical problems such as inability to work or perform daily activities but also develops mental illnesses as one becomes isolated from social activities. Rehabilitation is one of the most important aspects of the recovery, and the developed wearable assistance rehabilitation robot will aid not only the person but also a therapist to achieve the results wanted by the patient. The innovation of the developed robot is that it can be worn and easily transported, eliminating the need to attend medical institutions every time the rehabilitation training is needed. The robot frame was designed in order to withstand the required stresses and lightweight. The main material was selected to be the recyclable and biodegradable PLA plastic. For the production of this robot frame a 3D printing FDM method was chosen as an economically beneficial option. The motor-gear assembly as well as the motor controller were selected to ensure the required control of the robot. What is more, inductive proximity sensors for the position feedback were selected and a control algorithm was developed. A 3 point bending test using ISO:178 standard for plastics was conducted. 5 types of specimens ranging in infill density and infill geometrical pattern were tested. The results of the research showed that the best flexural stress resistance were achieved by using a solid infill and concentric infill geometry. However, reducing the infill by 40% only reduced the maximum flexural stress by 32.9 %, and the results were satisfactory for the robot frame application. The conducted research opened a possibility to reduce the robot frame weight by 40% and maintaining the required flexural strength. The novel wearable assistance rehabilitation robot was successfully designed in order to ameliorate the rehabilitation process for the patients with upper limb disability.

Patrikas Tatariūnas. Dėvimo pagalbinio roboto skirto rankos reabilitacijai kūrimas. Magistro baigiamasis projektas, vadovas Prof. Egidijus Dragašius; Kauno technologijos universitetas, Mechanikos inžinerijos ir dizaino fakultetas.
Studijų kryptis ir sritis (studijų krypčių grupė): Gamybos inžinerija (E10), Inžinerijos mokslai (E).

Reikšminiai žodžiai: viršutinės galūnės reabilitacija; dėvimas pagalbinis robotas skirtas reabilitacijai; PLA plastikas; 3D spausdinimas naudojant FDM technologiją; ISO:178 tritaškis lenkimo testas.

Kaunas, 2023. 52 p.

Santrauka

Viršutinės galūnės motorinės funkcijos sutrikimą gali sukelti daugybė dalykų, įskaitant sporto traumas, nelaimingus atsitikimus, sveikatos problemas ar insultus. Šios negalios paveiktas asmuo susiduria ne tik su fizinėmis problemomis, tokiomis kaip nesugebėjimas dirbti ar atlikti kasdienės veiklos, bet ir suserga psichinėmis ligomis, atsiribodamas nuo socialinės veiklos. Reabilitacija yra vienas iš svarbiausių sveikimo aspektų, o sukurtas dėvimas pagalbinis reabilitacijos robotas padės ne tik pačiam žmogui, bet ir terapeutui pasiekti paciento norimų rezultatų. Sukurto roboto naujovė yra ta, kad jį galima nešioti ir lengvai transportuoti, todėl nebereikės lankytis gydymo įstaigose kiekvieną kartą, kai prireikia atlikti reabilitacijos pratimus. Roboto rėmas buvo sukurtas taip, kad atlaikytų reikiamus įtempius ir būtų lengvas. Kaip pagrindine medžiaga buvo pasirinktas perdirbamas ir biologiškai skaidomas PLA plastikas. Šio roboto rėmo gamybai buvo pasirinktas 3D spausdinimo FDM metodas kaip ekonomiškai naudingas gamybos būdas. Variklio-reduktoriaus mazgas ir variklio valdiklis buvo parinkti taip, kad užtikrintų reikiamą roboto valdymą. Be to, padėties grįžtamajam ryšiui parinkti indukciniai artumo jutikliai ir sukurtas valdymo algoritmas. Buvo atliktas 3 taškų lenkimo bandymas pagal ISO:178 standartą plastikams. Buvo išbandyti 5 tipų bandiniai, kurių užpildo tankis ir užpildo geometrinis raštas buvo skirtingi. Tyrimo rezultatai parodė, kad geriausias atsparumas lenkimo įtempiams buvo pasiektas naudojant vientisą užpildą ir koncentrinę užpildymo geometriją. Tačiau sumažinus užpildymą 40 %, didžiausias lenkimo įtempis sumažėjo tik 32,9 %, o rezultatai buvo patenkinami roboto rėmo gamybos naudojimui. Atliktas tyrimas atvėrė galimybę roboto rėmo svorį sumažinti 40% ir išlaikyti reikiamą lenkimo stiprumą. Naujas nešiojamas pagalbinis reabilitacijos robotas buvo sėkmingai sukurtas siekiant pagerinti pacientų, turinčių viršutinių galūnių negalią, reabilitacijos procesą.

Table of Contents

List of Figures

List of Tables

Introduction

The upper limb disability is a common problem and can happen because of the sport injuries, health related problems, accidents or strokes. Strokes in fact, are one of the leading causes of this disability. A stroke survivor may experience major repercussions such as trouble communicating, motoric muscle dysfunction, cognitive and sensory issues. As a result, stroke is categorized as a severe and potentially fatal condition. The impairment has a detrimental influence not only on the person's daily life routine and work performance, but also on the person's participation in communal activities and reintegration into former life habits prior to disability. This rapid transition from normal everyday living to impaired lifestyle leads to significant psychological diseases such as sadness and anxiety. After a stroke, a person's physical and mental issues can pile up quickly, and he or she may lose enthusiasm in the rehabilitation process, which is critical for recovering control of lost motor abilities. If a stroke survivor receives adequate therapy, he has a fair chance of regaining motor ability. Occupational therapy (OT) is one of the most common rehabilitations used to help patients. OT is a collection of activities and exercises performed with the assistance of a trained therapist. A stroke survivor and a therapist can accomplish great outcomes over time if done correctly and consistently, including being able to conduct basic everyday tasks such as dressing, eating, and general movement that a person could not do previously. However, OT has various issues since it is difficult to provide consistent outcomes when all OT therapists have varied levels of certification, which has a direct influence on the rehabilitation process. Furthermore, the best benefits are obtained when the therapy is as intense and consistent as possible, but the requisite intensity is seldom accomplished because it is greatly dependent on the person and one's resolve. To administer this issue novel mechatronic devices are being incorporated to the rehabilitation training. In many aspects, this integrated rehabilitation strategy is preferable. To begin with, typical OT activities may be performed with excellent reproducibility and engagement by attaching robots to the upper limb. These mechatronic gadgets help the patient accomplish motions, making rehabilitation more successful and interesting. Furthermore, the rehabilitation process may be properly followed with the assistance of unique control algorithms and sensors, and the plan can be altered personally based on the obtained data. In this approach, using cutting-edge technology, a patient can receive quality therapy that has a direct influence on his or her healing process. Nonetheless, therapists are given a valuable instrument to analyze the stages of recovery and enhance recovery plans while the patient is training. Rehabilitation automation is critical for the healing process and increases the quality of life for both patients and therapists. The proposed wearable assistance rehabilitation robot not only helps the patient and the therapist as described but also is novel in a way that it is compact and wearable, meaning the person will not need to the nearest medical institution to receive the rehabilitation training. This research opens a possibility for more accessible rehabilitation training methods that can help in the recovery process of the disabled patient.

Aim: to develop a wearable assistance rehabilitation robot for patients with upper limb disability.

Tasks:

1. to analyse different types and control methods of existing assistance robots for upper limb rehabilitation;
2. to design the frame for wearable assistance rehabilitation robot and perform stress analysis;
3. to integrate applicable electronic components for control of the wearable assistance rehabilitation robot;

4. to perform a research on mechanical properties of 3D printed specimens from PLA for the wearable assistance rehabilitation robot frame;
5. to evaluate social, environmental and economical aspects of wearable assistance rehabilitation robot;

Hypothesis: 3D printed wearable rehabilitation robot frame will be functional, lightweight and will withstand the required stress.

1. Analysis of mechatronic upper limb rehabilitative robots

Rehabilitative robots are aimed to aid people with upper limb disabilities and increase the quality of life by improving the rehabilitative process that is usually a hard and tiring journey towards a recovery. Before developing an upper limb rehabilitative robot, it is important to understand the difficulties that disabled people face and the scale of the problem.

1.1. Upper limb disability and rehabilitation

Upper limb motoric function disorder can be caused by numerous reasons, including sport injuries, accidents, health related problems or strokes. However, a stroke is one of the leading causes of this disability. Stroke is described as a brain injury that is caused by a breach or damage of a blood vessel. Data shows, that almost 3 million people are affected yearly and a chance of disability after a stroke can reach up to 75% [1]. A person who survived the stroke may have serious consequences, such as difficulty to communicate, motoric muscle dysfunction, cognitive and sensory problems. That is why stroke is classified as a serious and life threatening case. The disability not only has a negative impact on the person's daily life routine, working performance but also participation in communal activities and reintegration to previous life habits before disability. This fast shift from normal daily life to impaired lifestyle also causes severe psychological illnesses such as depression and anxiety. The cluster of physical and mental problems that one face after a stoke can come in total extremely fast and a person may lose the motivation in rehabilitation process that is vital for regaining control of motoric skills that were lost. If a stroke survivor is provided with proper rehabilitation, then there is a good chance for him/her to recover motoric abilities. One of the most popular rehabilitations in order to assist the patient is occupational therapy (OT). OT is a combination of various activities and exercises that are practiced with the help of a qualified therapist. If done correctly and continuously a stroke survivor and a therapist can achieve great results over time, including being able to do basic everyday activities such as dressing, eating, general mobility that a person could not do before. However, OT has several problems as presented in Fig. 1. First of all, it is hard to ensure similar results when all the OT therapists have different levels of qualification and it directly impacts the process of rehabilitation.

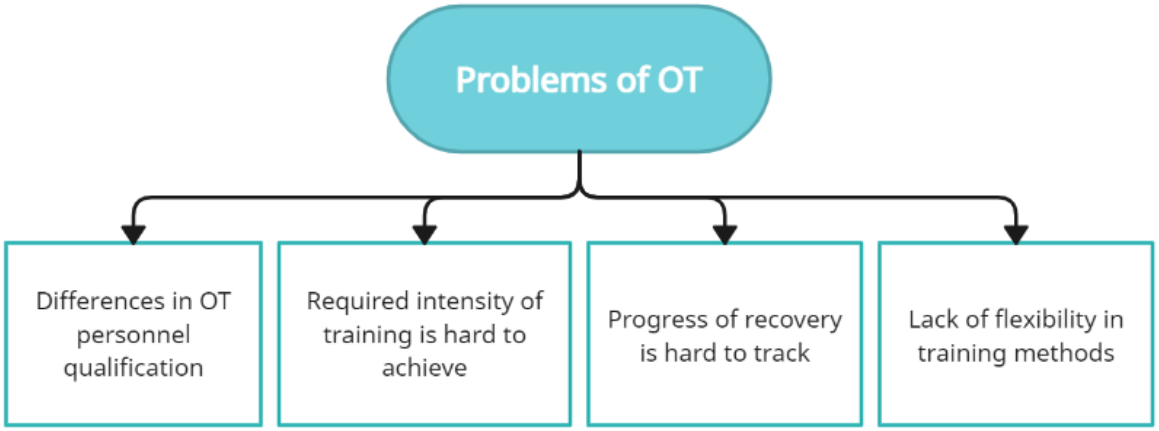

Fig. 1. General problems of occupational therapy

Additionally, the best results are achieved when the therapy is as intense and regular as possible, but the required intensity can rarely be achieved as it highly depends on the person and one's determination. What is more, the results of the patient's progress in OT can only be determined by visual help, for example if a person is able to do a movement that one was not able before, however this progress can take a long time and there are no tools to determine if the direction of recovery is correct or the program needs changing. Lastly, as OT usually requires professional therapist, and it is usually performed in medical institutions meaning a person cannot receive the proper training at home. In account the recent COVID-19 outbreak, people had to omit OT for months or in other cases years as they were not able to come to the nearest medical institutions. This outbreak has shown the lack of flexibility of the OT and the need for an alternative that a stroke survivor could continue his rehabilitation at home if a direct contact with therapist is impossible or limited [2-4].

1.2. Automatization of rehabilitation process

Robots are helping people in numerous cases every day, whether it is in automotive applications, production industry, aeronautics or medicine. To tackle the named problems and aid not only patients in successful recovery but also provide a tool for therapist to grant the best possible therapy services mechatronic robots were introduced to the rehabilitation process. Rehabilitation with the help of robots as presented in Fig. 2, is a combination of OT exercises and practices and novel mechatronic technologies.

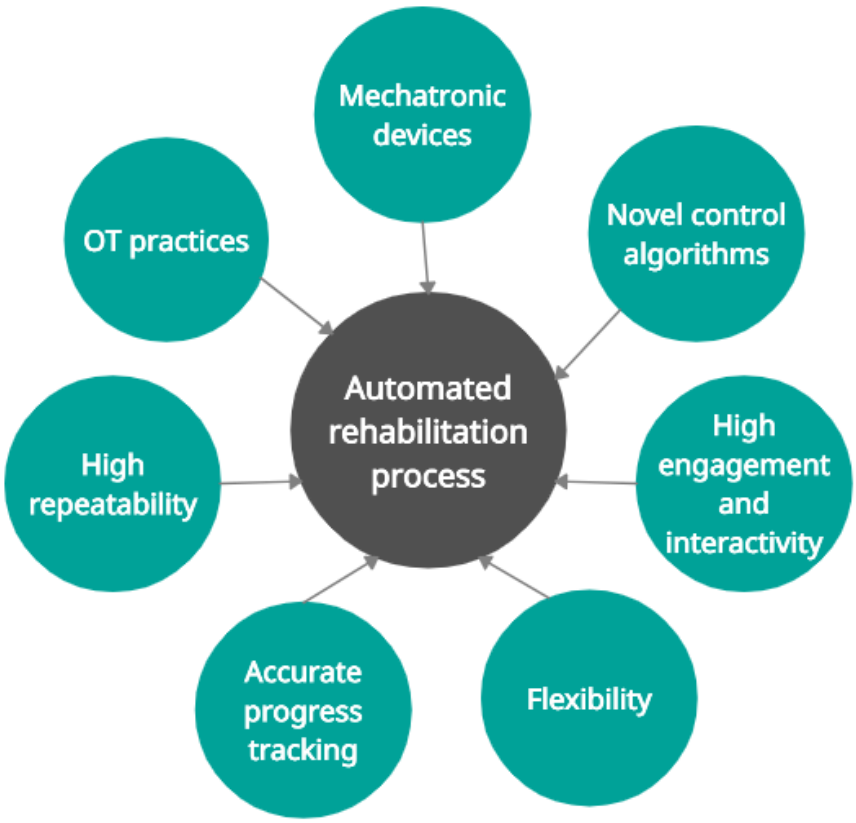

Fig. 2. Automatization of rehabilitation process

This combined rehabilitation method is superior in many ways. First of all, regular OT exercises can be done with high repeatability and engagement using robots that can be attached to the upper limb. These mechatronic devices aid the patient in performing movements and thus makes the rehabilitation process more successful and enjoyable. What is more with the help of novel control algorithms and sensors, the rehabilitation progress can be accurately tracked, and the plan can be adjusted personally according to the gathered data [5-7]. In this way, with the help of state of the art technologies a patient can get qualitative rehabilitation that is directly making impact on one's recovery process. Nevertheless, therapist are provided with a powerful tool to analyse the recovery stages and improve recovery programs as the patient is training. Automatization of rehabilitation is vital for the recovery process and improves quality of life for both patients and therapists.

Scientists from Belgium have conducted an experiment to determine the effectiveness of robotic aided rehabilitation in comparison to conventional therapy. 45 patients were divided into two groups. The first group were training with the help of conventional therapy, however the second group had 25% of training converted to robotic assisted therapy, meaning they had a robot that would assist them in their trainings. The experiment lasted 9 weeks and several criteria were taken into account: results in motor control, manual activity, social participation, ability of everyday activities and others [8]. The results of an experiment can be seen in Fig. 3.

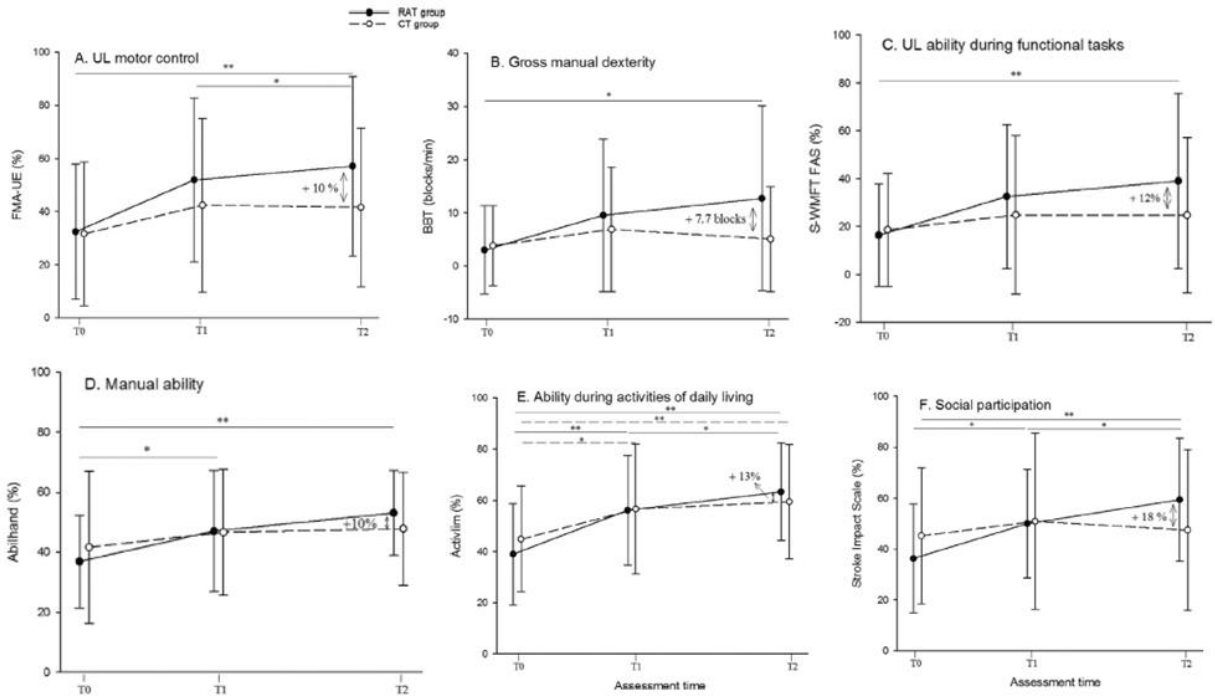

Fig. 3. Results of the conducted experiment (dashed line – first group, bold line – second group) [8]

As seen from Fig. 3, results show that there was an increase in performance (10-18%) of all activities in group 2, that was training with the help of robot. That means that rehabilitation process with robot assistance is more effective for patient with upper limb disability compared to only conventional therapy.

1.3. Types of mechatronic rehabilitative robots

In general, rehabilitation robots are divided into two main groups based on their mechanical structure: end-effectors and exoskeletons (see Fig. 4.). End-effectors are connected to a person at single distant point and joint position does not match with patient's joints. When the force is generated at the distant point it changes the position of all connected joints at the same time, meaning the single movement of joint is difficult to achieve. On the other hand, exoskeletons copy person's limbs and the joints are connected at several points the patient's limb to match the joint axes. This mechanical structure allows training a specific muscle group by controlling joint movements with desired torque [9].

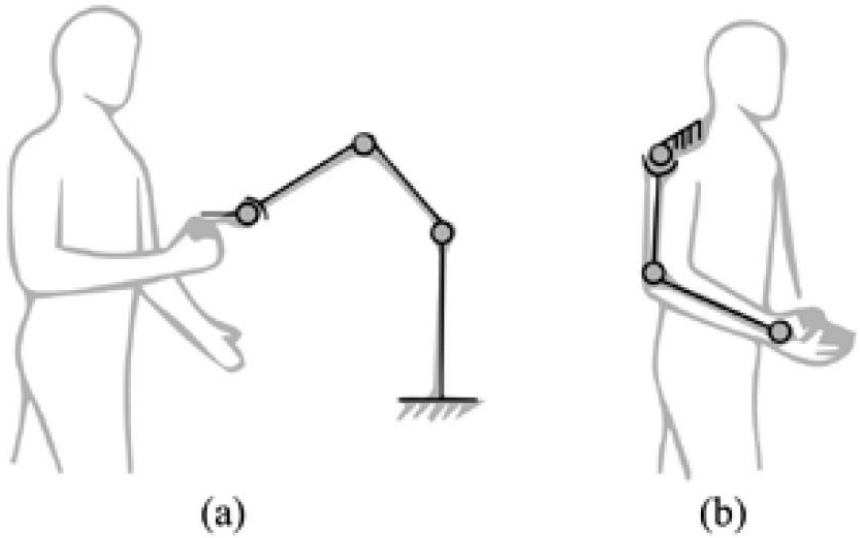

Fig. 4. Schematics of main rehabilitation robots: a) end-effector and b) exoskeleton [10]

Both types of rehabilitation robots are widely used to aid patients with upper limb disabilities. It is important to analyse the differences and possibilities in order to select the type for the final study.

1.3.1. End-effector upper limb rehabilitation robot (EULRR)

Scientists from China have developed a novel upper limb robot for rehabilitation. The robot aims to aid patients with upper limb dysfunction in spatial trajectory rehabilitation training. What makes this robot unique is two integrated manipulators allowing to train both hands at the same time or one at once. General model of the rehabilitation robot is presented in Fig. 5. The physical structure unit and the mobility aid component are the two core sections of EULRR. The physical construction module, which has six universal wheels, primarily serves to support the aid mobility module, in addition to the robot controller cabinet, command computer, and electrical structure. The mobility assisting module, which is built of two industrial manipulators, is mounted outside of the body structural module and serves to support and aid the patient's hand in performing rehabilitation training. Every manipulator has 7 degrees of freedom, and every joint contains a torque sensor and a position encoder, which may be realized through torque control [11].

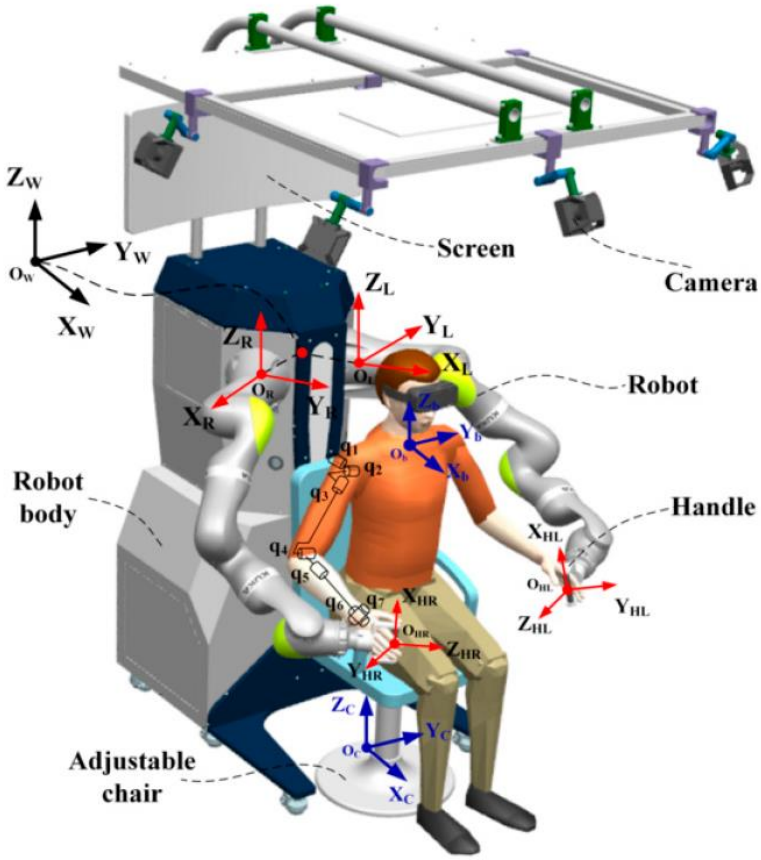

Fig. 5. Model of a novel end-effector for rehabilitation EULRR [11]

The manipulator's payload is 7 kg, and its operating range is 800 mm. Two grips are attached to the ends of the manipulators and are utilized to link the manipulator to the patient's wrist via the wrap [11]. The developed rehabilitation robot is very flexible and can help the patient in various rehabilitation activities. However, this robot is relatively expensive and not applicable for usage at home environment as it needs qualified personnel to operate it.

1.3.2. Shoulder joint rehabilitation mechanism based on gear and rack transmission

Another rehabilitation robot developed by researches from China is less complex and is based on gear and rack transmission (see Fig. 6). The construction of the rehabilitation system for shoulder joint recovery training is based mostly on peculiarities of the person's body shape and the characteristic of shoulder joint motion. The exoskeleton system is built of three major motion units and single passive adjustable module that is attached to the elevating base. These three major motion components are used to implement the shoulder joint's flexion/extension, internal/external rotation, and abduction/adduction movements, while the passive correction component accomplishes the joint's control function locally. The harmonic reduction actuator drives and connects different sections of the system in the 2-DOFs of flexion/extension and abduction/adduction motions. Nevertheless, the DOFs of inside/outside revolution that use the upper limb as the axis cannot utilize the construction above since the device must be worn, limiting its applicability. A round arc slider is built inside the raising station to eliminate this issue and contacts with the reducer's output spindle gear via an arc-shaped rack on the round arc slider rail powered by the motor driver. The round arc slider allows for inside/outside rotation of the shoulder joint [12].

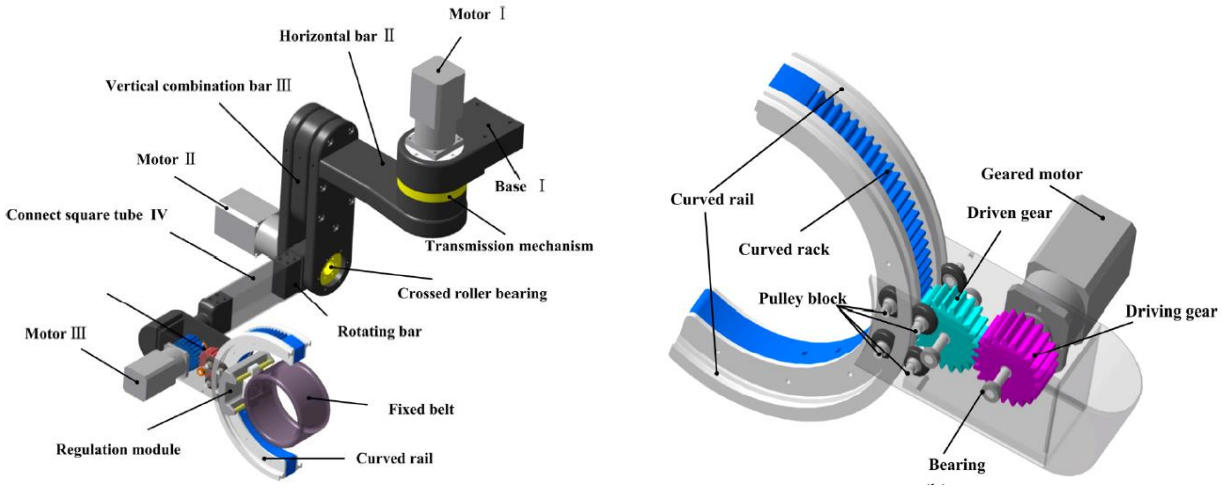

Fig. 6. Schematics of rehabilitation robot with gear rack transmission [12]

Two pairs of rollers are attached on either ends of the arc rack to restrict the arc guiding rail, and a passive gear is constructed in between drive gear and the arc rack to minimize the motor's output torque and system weight. Because arms are built at both sides of the arc rack, the passive gearing may solely connect with the arc rack inside a specified range of angles, ensuring the patient's security. The preventive measure is to restrict the range of movement of the shoulder joint's revolution by adjusting the amount of slots of the passive gear and the arc rack [12]. Reviewed rehabilitation robot is more compact than the last one and is relatively less expensive. Nonetheless, it still needs a base that it should be attached to meaning the patient could not wear it on the upper limb.

1.3.3. Variable stiffness joint for rehabilitation exoskeleton

Robotic joints with built-in compliance can be employed in rehabilitation equipment. In general, flexible joints are used to enhance the security of physical human interaction, increase dynamic mobility with the environment, and boost energy efficiency. There have been several suggestions for flexible joints with varied stiffness characteristics. They are classified as fixed compliance joints or adjustable compliance joints. Linear springs and stiff motors are frequently used in fixed compliance joints. Adjustable compliance joints, as opposed to fixed compliant joints, may change stiffness dynamically. They may be made with a number of approaches, such as spring preload, transmission rate, and custom springs. The design approach is to provide changeable stiffness through a variety of modes whilst simultaneously enabling rigidity changes easy. By modifying the design preload, variable stiffness may be achieved, and three working modes with hardening, softening, and linear behaviours can be performed. Additionally, the mechanism-based changeable design is offered to easily ease the modification of its stiffness and output torque restrictions. The variable stiffness mechanism is built with two coaxial shafts: input and output shafts that are linked by a cable-pulley-spring system as shown in Fig. 7. The worm gear of the variable stiffness mechanism is linked to a cable roller to control the cable pretension [13].

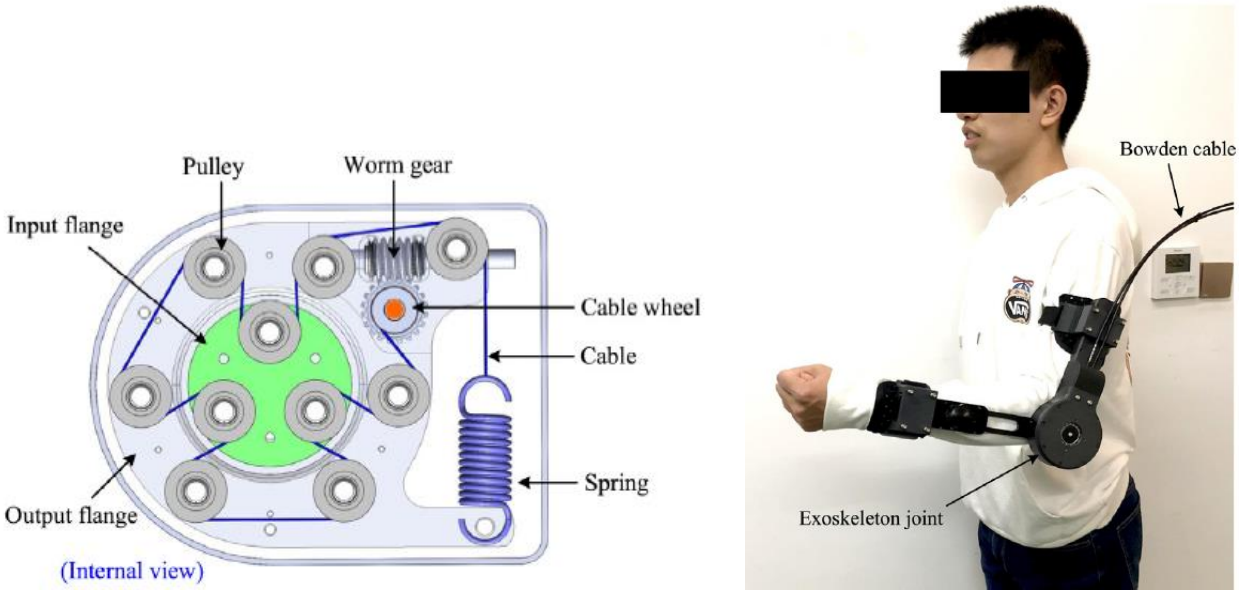

Fig. 7. Model of variable stiffness joint and application in rehabilitation exoskeleton [13]

The novel variable stiffness joint is a great option for compact and wearable exoskeletons. It does not require complex mechanical structure nor great expenses. However, this variable stiffness joint is applicable for passive training, meaning it provides passive resistance training for patients with upper limb disability. It is an excellent option for the patients who are advanced in their rehabilitation process, but the early stage patients require active training as well as they do not have enough force to complete exercises without any help.

1.4. Control methods for rehabilitation robots

Rehabilitation robots' control is dependent on the control algorithms. These algorithms take into account the current state of the upper limb: angle, velocity, torque and calculate what the robot should do and how it should move. Novel algorithms are the key to successful rehabilitation as they can be configured to adapt to different needs of patents. It is important to cover different control methods in order to understand their working principle.

1.4.1. Assistance as needed control algorithm TPAVAAN

Collaboration of scientists from China and Italy, have developed a novel control algorithm for rehabilitation end-effector. The main advantage of this control algorithm is that it calculates how much assistance is needed for the patient to perform the task and provides exactly the required force. In this way the patient can train and perform task successfully and progress faster in rehabilitation process. The control scheme of this algorithm can be seen in Fig. 8.

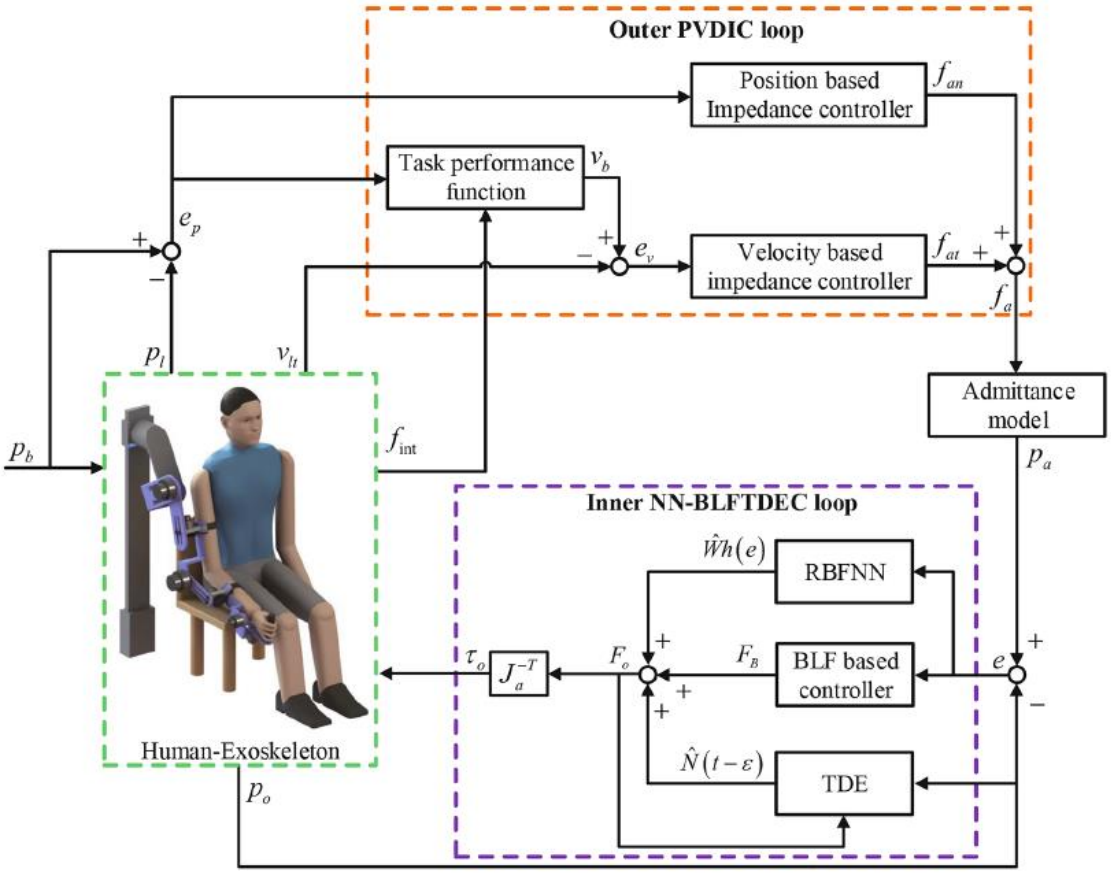

Fig. 8. Control scheme for assistance as needed control algorithm TPAVAAN [14]

An outer PVDIC loop as well as an inside NN-BLFTDEC loop are part of the TPAVAAN control scheme. The PVDIC is created to calculate the needed assistance force, while the NN-BLFTDEC is meant to have the exoskeleton track the patient's motion and supply the PVDIC-determined supportive force. The standard supportive force is calculated using a position-based impedance regulator in PVDIC, while the tangential supportive force is calculated using a velocity-based impedance regulator. To assess the patient's physical competence, an individual task function based on positional monitoring inaccuracy and standard supportive force is presented. The target speed is modified dynamically depending upon it. The goal supportive force is finally translated into the target path employing an admittance concept, and the NN-BLFTDEC is developed to manage the exoskeleton that maintains the guide direction. A BLF is used in this system to ensure that the exoskeleton monitoring inaccuracy is restricted, whereas the TDE technique and RBFNN are used to simulate the unpredictable exoskeleton dynamics [14]. The developed control technique is novel and widely applicable for end-effectors in rehabilitation.

1.4.2. Torque control system for exoskeleton

Researchers from Poland have developed a control system for Bowden cable driven rehabilitation exoskeleton as depicted in Fig. 9. The transmission mechanism depicted inside the closed-loop wire conduit arrangement for the exoskeleton part incorporates force and torque sensors into its design that are placed in every joint. The sensor monitors the cumulative influence of the equipment parts' motion, gravitational loads, as well as the contact torque with the equipment user, which is an unfavourable feature of such approach. To calculate the interface torque from the observed data, it

is necessary to subtract the objects kinematics value from the recorded signal. This metric is obtained employing a Newton-Euler iterative dynamics framework. To compute the torque given to a rotating connection owing to element motion and force of gravity, the angular location of every component, along with speed and acceleration, must be known. The LS filter technique is used to derive this result out from angular orientation [15].

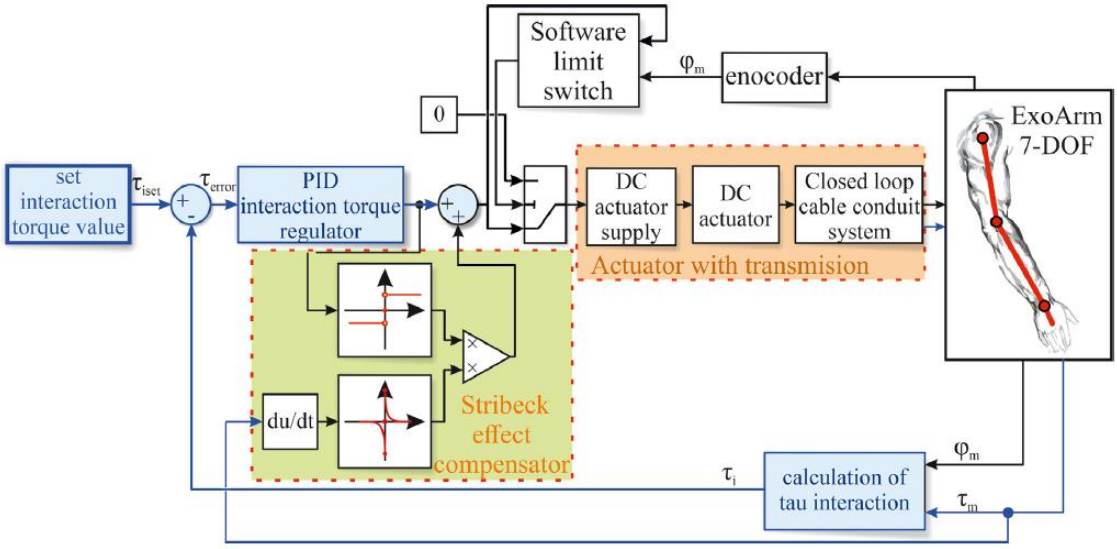

Fig. 9. Torque control system for upper limb rehabilitation exoskeleton [15]

The linear actuator's DC motor in the driving mechanism is operated by varying its extension speed. The use of cable mechanism in the transmitting system causes severe non-linearities into the joint's performance. The influence of contact pressures is most obvious whenever the vector of motion of the connection changes. When the joint is redirected, a substantial blind spot is detected. A contact correction unit was added in the controlling scheme to reduce this impact. After assessment of several friction compensating techniques in wire structures, the Stribeck effect compensator produced the greatest outcomes [15].

1.4.3. Summary

After reviewing several rehabilitation robots and their use of application it can be seen that end-effectors are usually large in dimensions and have a complex structure. This type of robots is an excellent choice for medical institutions to provide best rehabilitation services for patients as end-effectors usually also require personnel to monitor the work. On the other hand exoskeletons are more compact and can even be worn on the upper limb without any additional mounting to the ground. Even more, exoskeletons allow the movement of specific single joint meaning more adaptive and accurate training can be achieved. The difference in the working principle is if the exoskeleton adapted for active or passive training. Active training is more useful for patients in early stages of rehabilitation as a person needs additional help from the exoskeleton to perform the exercises. Hence, for the final theses an active exoskeleton model was chosen which should be compact, wearable on the upper limb and could be used for daily exercises at home. After analysing several control algorithms for end-effectors and exoskeletons a conclusion was drawn that a vital part for successful control is the feedback from sensors. This data collected from sensors then can be processed and response is then calculated as what the robot should do to aid the patient's movements. Angle and torque sensors will be used in the final work alongside the assistance when needed control algorithm to achieve the best results.

2. Development of a wearable assistance rehabilitation robot

Before developing a rehabilitation robot for an upper limb, it is important to understand it's anatomy and kinematics and calculate important parameters for the research.

2.1. Anatomy and kinematics of the upper limb

The upper limb extremity consists of shoulder and elbow complexes as shown in Fig. 10. The shoulder complex is made up of the scapula, humerus, clavicle, and multiple joints, including the sternoclavicular (SC) joint, acromioclavicular (AC) joint, scapularthoracic (ST) joint, and glenohumeral (GH) joint. Research on upper limb biomechanics has revealed that the motion of the shoulder complex is comparable to three DOFs in the motion of the GH joint with a floating rotating centre. The revolution of the humerus along its axis is unrelated to shoulder girdle motion, but revolution in the opposing two axes is connected to shoulder girdle motion, leading in variations in the location of the GH joint's rotary point. As a result, the shoulder complex is seen as a 3-DOF spherical joint with a floating rotating centre, allowing adduction-abduction, flexion-extension, as well as internal-external motions around the GH joint [16].

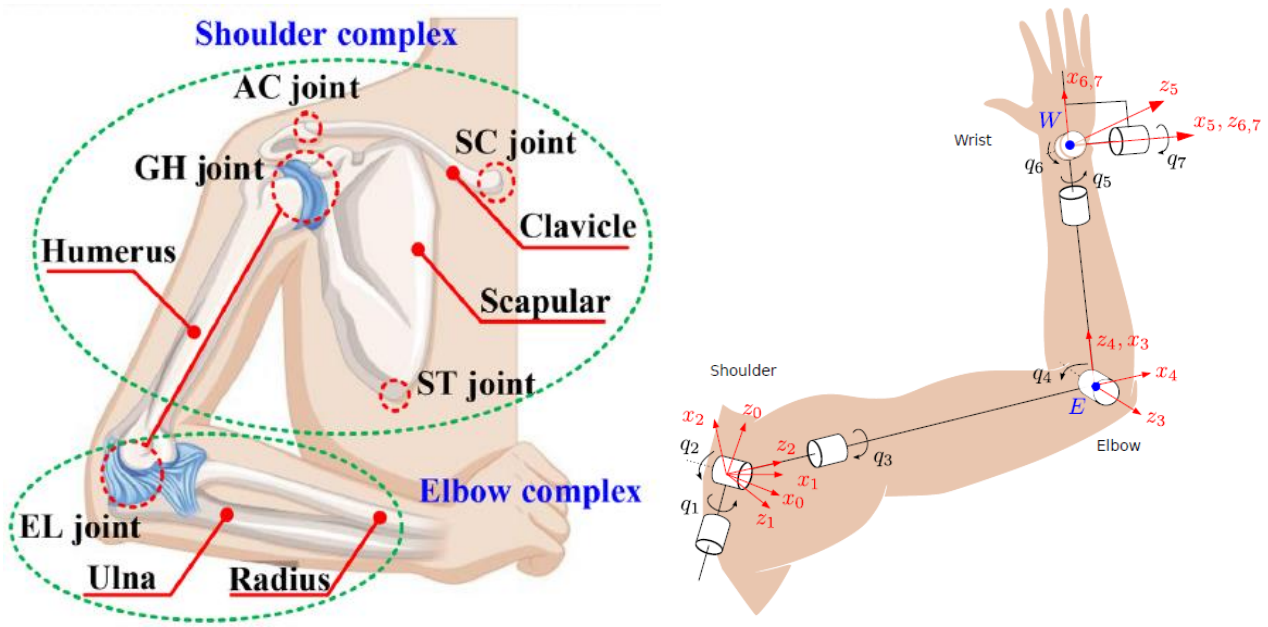

Fig. 10. Anatomy and kinematic model of an upper limb complex [16,17]

The elbow (EL) complex is made up of the humerus, ulna, radius, and EL joint. According to studies, the EL joint is a 2-DOF hinge joint that can rotate and translate. Nevertheless, because translational displacement measurements are fairly tiny, translational motions are often neglected in the EL joint model. As a result, the EL joint is a 1-DOF revolute joint [16].

For the final project assistive rehabilitation robot for the elbow joint is selected. Before the development of robot, three main parameters have to be analysed: maximum and minimum position angle of elbow joint, angular velocity and torque. For the determination of maximum and minimum position angles, an experiment was conducted in KTU biomechatronic laboratory using a measurement tool – protractor as shown in Fig 11. The results show that the maximum angle that the elbow joint can bend is 180 deg, while the minimum is 50 deg. These angles will be the limits for the assistive rehabilitation robot in order not to harm the patient during the training.

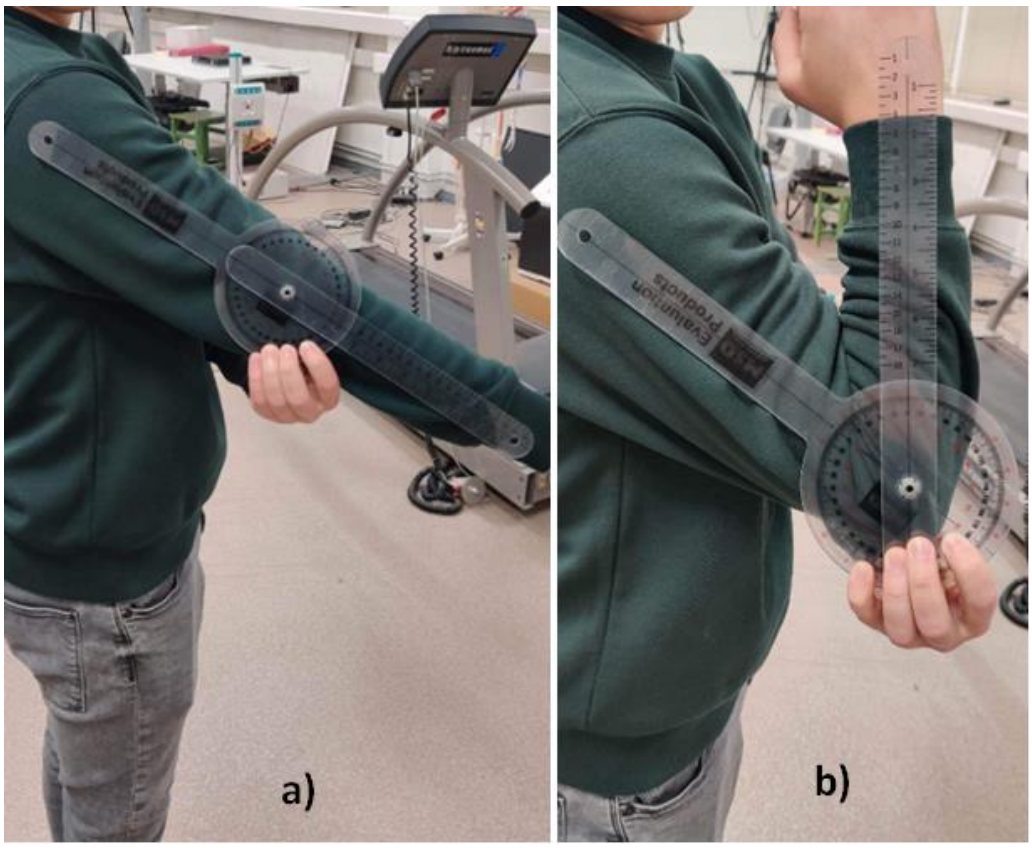

Fig. 11. Maximum a) and minimum b) elbow joint angle

In order to determine the angular velocity of the elbow joint a test with three different speeds was performed. The starting position of the elbow was in the maximum position and the elbow was moved to the minimum position while tracking the time that it took. The first speed was the slowest, imitating the rehabilitation training, second was the speed that the elbow is moving during everyday tasks, for example: picking up the cup of tea. The third one was to bend the elbow as fast as possible to determine the maximum velocity. The results are depicted in Table 1.

Table 1. Results of an elbow joint movement with different speeds

Speed of elbow joint movement	Time, s
Rehabilitation training	7.2
Every day activity	2.8
Maximum speed	0.3

The angular velocity can be calculated as follows:

$$\omega = \frac{\alpha_{max} - \alpha_{min}}{t}$$

where: ω is the angular velocity (deg/s); α_{max} is the maximum angle of the elbow joint (deg); α_{min} is the minimum angle of the elbow joint (deg); *t* is time (s).

$$\omega_1 = \frac{180 - 50}{7.2} = 18.1 \ deg/s$$

$$\omega_2 = \frac{180 - 50}{2.8} = 46.4 \ deg/s$$
$$\omega_3 = \frac{180 - 50}{0.3} = 433 \ deg/s$$

After the calculations, it can be seen that the elbow joint can achieve angular velocity in the range from 18.1 to 433 deg/s. These values will be important for developing the control mechanism as the training and limit values of the angular velocity.

Lastly, the torque of the elbow joint needs to be calculated. For these calculations the mass and the length of the forearm must be known. Scheme for calculations is shown in Fig. 12.

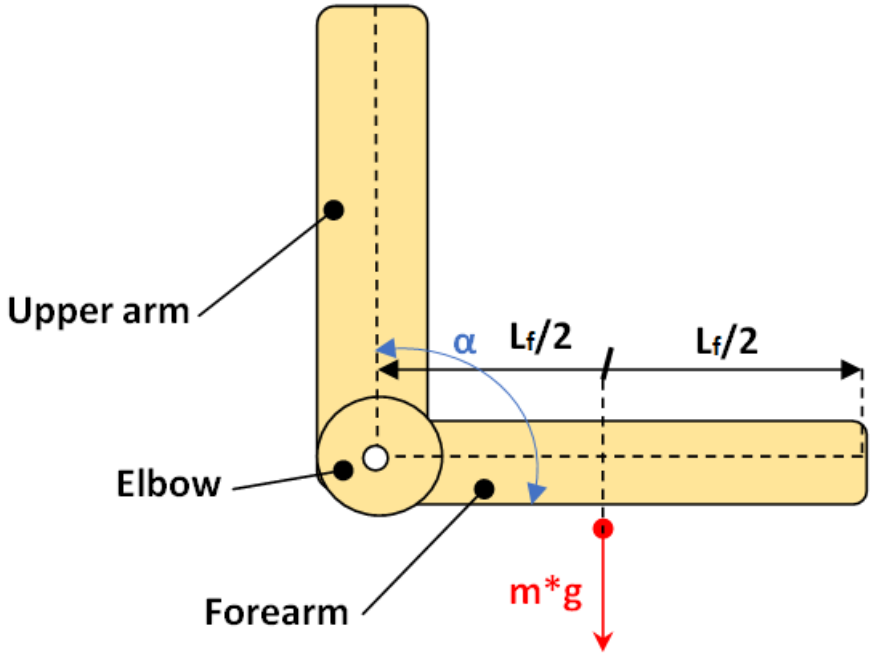

Fig. 12. Scheme of an upper limb

The mass of forearm can be calculated from table 2:

Table 2. Segment weights as percentage of body weight [18]

Segment	Percentage of body weight
Head and neck	7.6
Torso	4.2
Upper arm	3.2
Lower arm	1.7
Hand	0.9
Thigh	11.9
Calf	4.6
Foot	2.0

While the length of the forearm can be calculated from table 3:

Table 3. Segment lengths as percentage of body length [18]

Segment	Percentage of body length
Head and neck	10.75
Torso	30.00
Upper arm	17.20
Lower arm	15.70
Hand	5.75
Thigh	23.2
Calf	24.7
Foot	14.84

The torque of the elbow joint can be calculated with a formula:

$$T = m * g * \frac{L_f}{2}$$

where: T is the torque of the elbow joint (Nm); m is the mass of the forearm; L_f is the length of the forearm (m); g is gravitational acceleration constant (9.8 m/s^2);

Using the torque formula and data from tables 2 and 3, torque calculation for different mass and height of people are performed and result depicted in table 4:

Table 4. Results of elbow joint torque with different mass and heights

	150 cm	**160 cm**	**170 cm**	**180 cm**	**190 cm**
60 kg	2.35	2.51	2.67	2.82	2.98
70 kg	2.75	2.93	3.11	3.30	3.48
80 kg	3.14	3.35	3.56	3.77	3.98
90 kg	3.53	3.77	4.00	4.24	4.47

The results and data for further development of rehabilitation robot can be seen in table 5:

Table 5. Kinematics data and calculated results of elbow joint for further development

Maximum angle	180 deg.
Minimum angle	50 deg.
Range of movement angle	130 deg.
Range of angular velocity	18.1 – 433 deg/sec
Range of torque	2.35 – 4.47 Nm

2.2. Design of a wearable assistance rehabilitation robot

Wearable assistance rehabilitation robot has several requirements that have to be noted before the design process. Firstly, it has to be lightweight, easily wearable and comfortable for the patient. Secondly the range of motion of the robot has to be limited from 50 to 180 deg. as mentioned in the table 5. The robot frame also has to withstand the forces of maximal 4.47 Nm torque that the person can reach and the control of the motor has to be configurable (speed and torque). Fig. 13. represents the concept of wearable assistance rehabilitation robot.

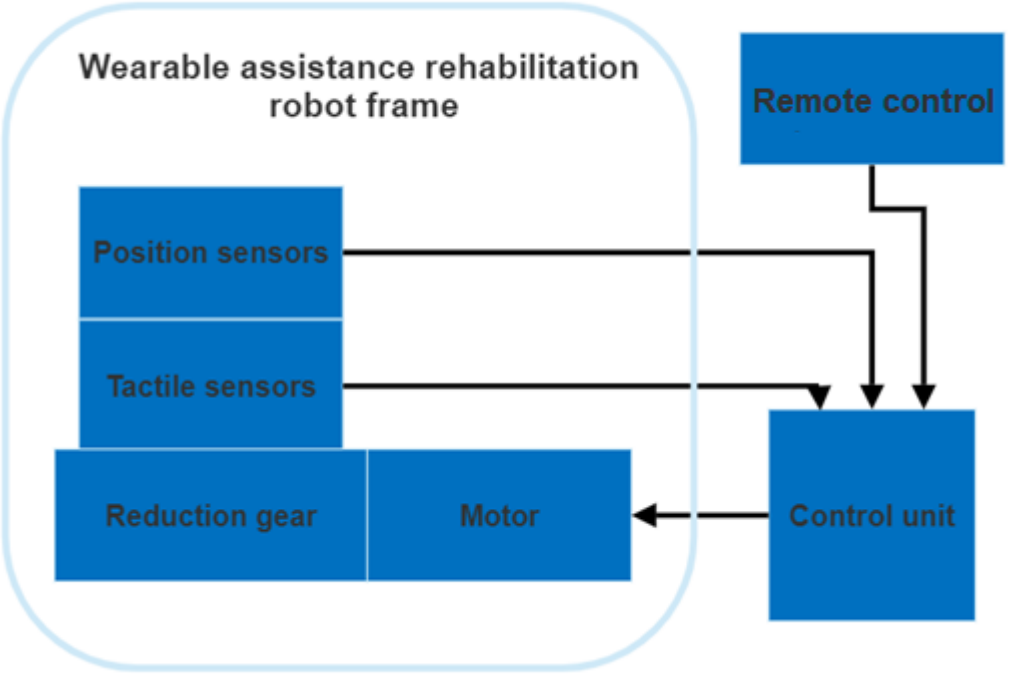

Fig. 13. Scheme of wearable assistance rehabilitation robot concept

As seen from Fig. 13. on the robot frame there will be mounted position and tactile sensors for the feedback. They are sending signals to the control unit that analyses the feedback data and send the command for the motor. A remote controller will be used to control the wearable assistance rehabilitation robot. Some predetermined parameters as maximum position angles, allowed angular speeds and torque, is written fort the control unit in order to assure safe and effective training. This chapter further covers the design and strength simulations of wearable assistance rehabilitation robot frame as well as motor and reduction gear application.

2.3. Modelling and design of wearable assistance rehabilitation robot frame

The designed frame for wearable assistance rehabilitation robot has to be lightweight, support the upper arm as well as forearm, have rotatable elbow joint, be comfortable for the wearer and withstand stress from the torque of the patient. The designed frame as well as all the main components can be seen in fig. 14. For the design of the frame Autodesk Inventor Professional 2023 software was used.

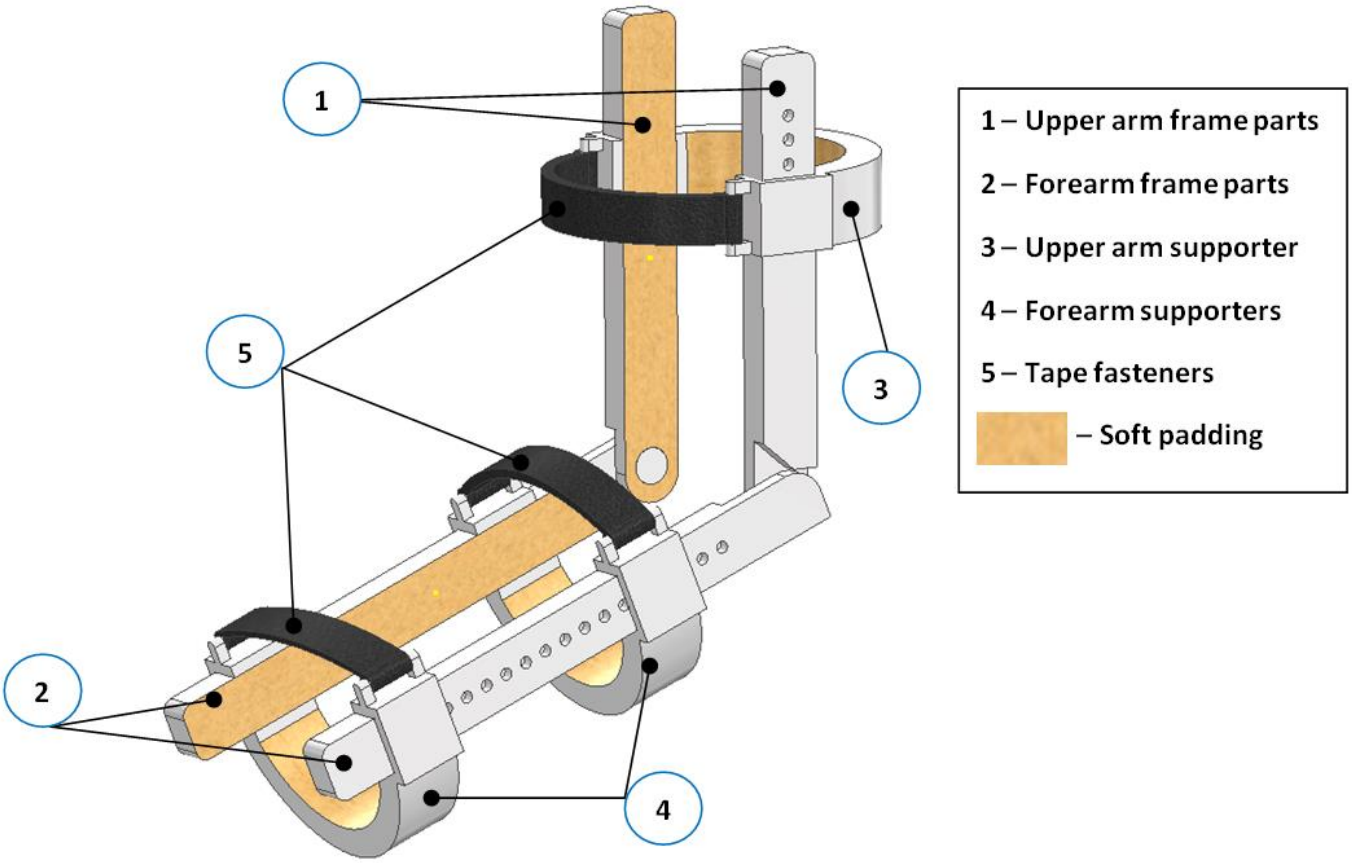

Fig. 14. Designed frame for wearable assistance rehabilitation robot

As can be seen from fig. 14. the frame for wearable assistance rehabilitation robot consists of 5 main types of components. Two upper arm frame parts support the upper arm with the help of upper arm supporter that is fixed to the frame parts and tightened with the help of tape fastener for convenient wear. The forearm is also held by using two forearm frame parts and two forearm supporters that are fixed and tightened the same way as the upper arm. Two supporters were chosen for the forearm as it is a longer part of the arm and to distribute the stress equally in order to minimize any inconvenience for the patient. The forearm and upper arm frame parts are connected with pins in the rotational axis and form a revolute joint for comfortable rotation of the elbow joint. Additionally all the surfaces that are in touch with the patient's arm will be covered with soft padding to ensure comfortable wear.

2.3.1. Upper arm frame parts

Upper arm frame parts for wearable assistance rehabilitation robot have to withstand the torque during the rehabilitation process that is described in table 5. The frame also has to support the arm and hold it in place in order to perform the training. Additionally, upper arm frame parts have to have pins at the rotational axis and a fixture point for the upper arm supporter. The upper arm frame parts were designed in Autodesk Inventor Professional 2023 software and stress analysis was performed using the stress analysis environment. The results can be seen in fig. 15.

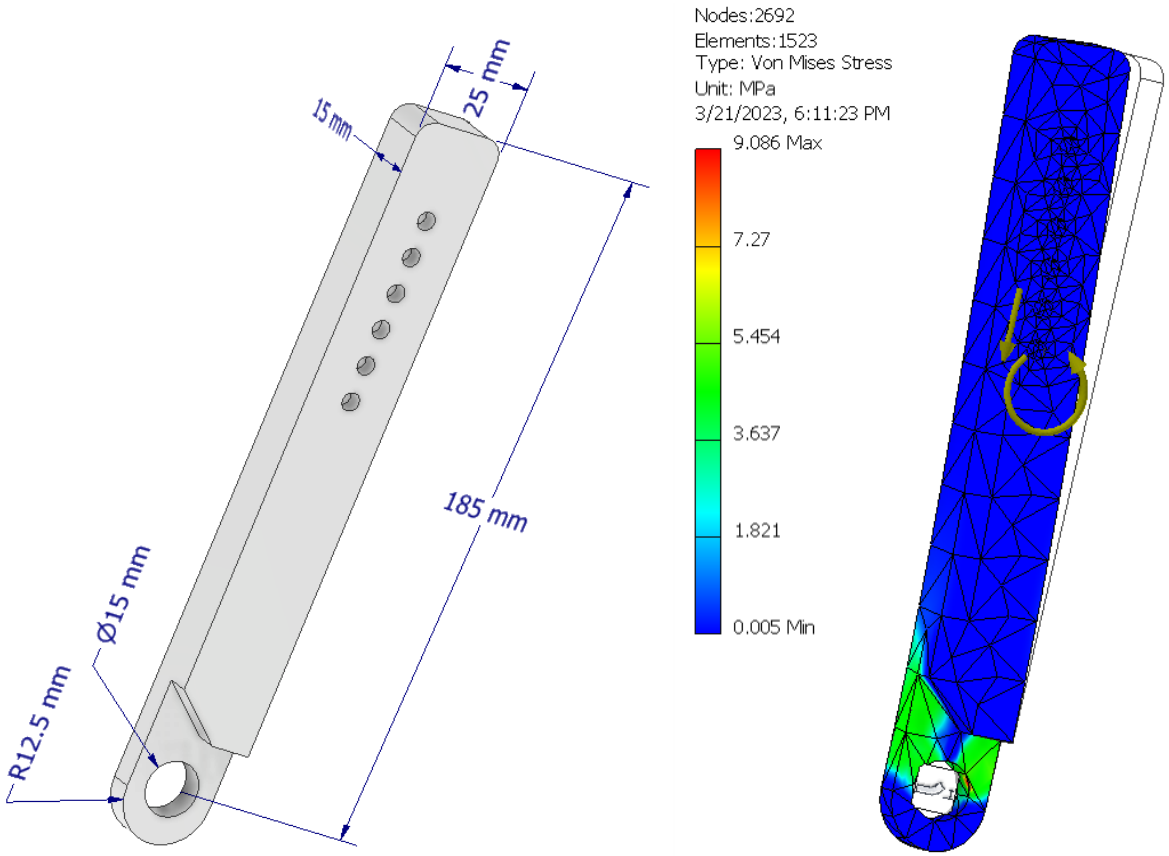

Fig. 15. General dimensions of the designed upper arm frame part and stress analysis results

For the stress analysis the fixed point was the pin hole, the maximum torque of 4.47 Nm and gravitational force was added. As can be seen from fig. 15. maximum Von Misses Stress was 9.09 MPa and the concentration of it was near the fixing point.

2.3.2. Forearm frame parts

Forearm frame parts for wearable assistance rehabilitation robot were designed (see fig. 16-17.) to withstand the torque of the patient's upper arm movements during rehabilitation. The frame has to support the forearm and keep it tight during the training. Two forearm supporters also mount on the frame, meaning fixing points for them have to be designed. The pin at the rotational axis point aids to rotate the wearable assistance rehabilitation robot.

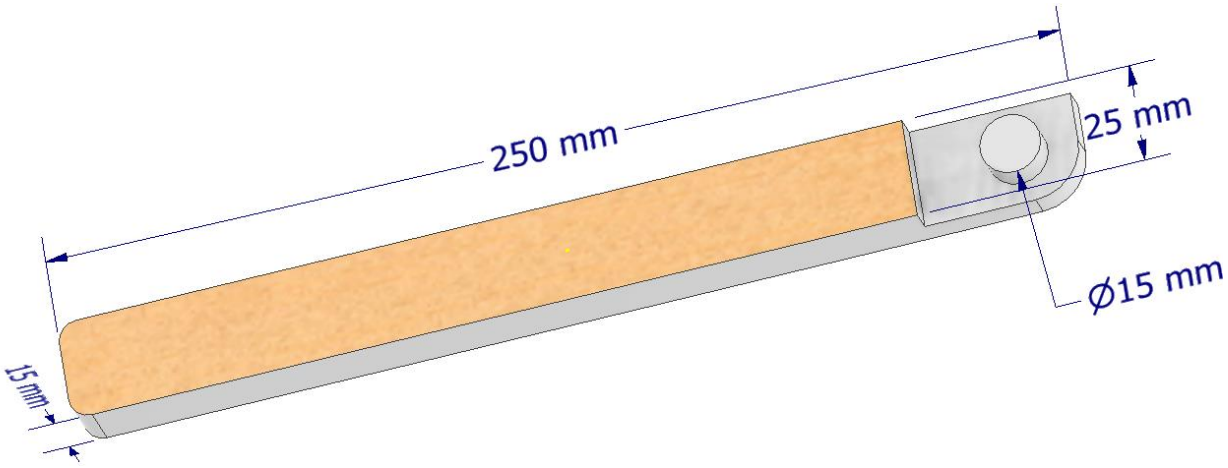

Fig. 16. General dimensions of the designed forearm frame part

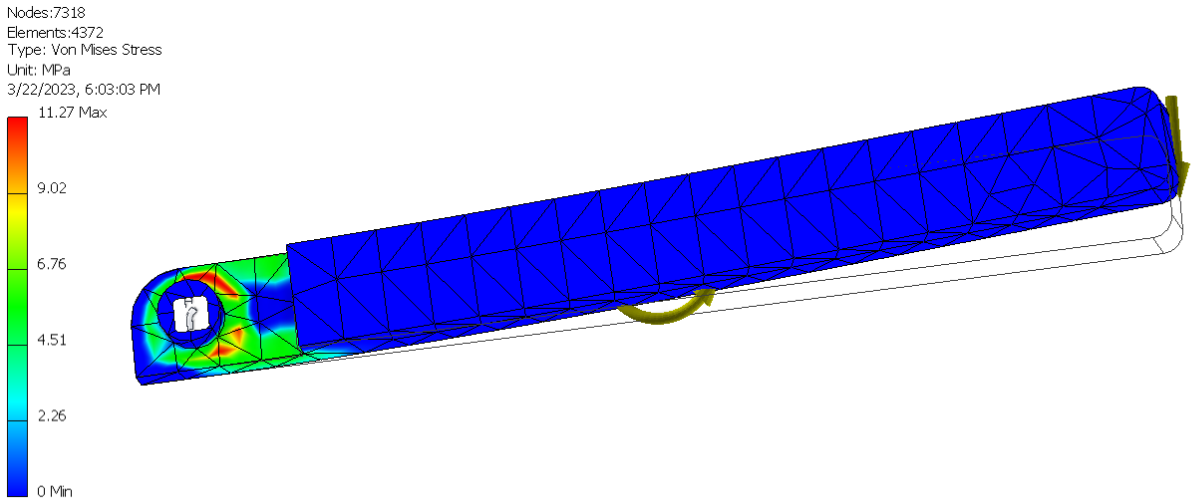

Fig. 17. Stress analysis results of the designed forearm frame part

Frame parts were designed in Autodesk Inventor Professional 2023 software and stress analysis was performed using the stress analysis environment. The fixed point was chosen to be the pin, maximum rotational torque was selected – 4.47 Nm and gravitational force applied. The results indicate the maximum Von Misses stress of 11.27 MPa and the stress is mostly distributed around the pin fixing points.

2.3.3. Upper arm and forearm supporters

Upper arm and forearm supporters connect the frame parts together. They all have different arcs that imitate the upper limb dimensions of the place they are supporting. They connect to the frame with three pins. At the top of both ends there is a fixing point for the tape fasteners. The tape fastener fixes to one end, wraps the arm, goes around the other end and attaches to itself. Supporters were designed in Autodesk Inventor Professional 2023 software and stress analysis was performed using the stress analysis environment as can be seen is fig. 18-19.

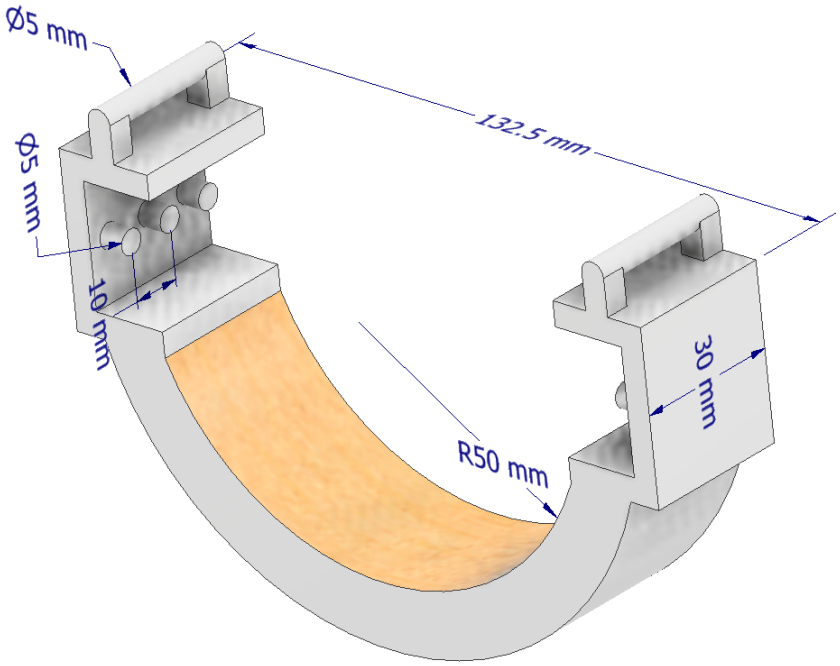

Fig. 18. General dimensions of the designed supporter

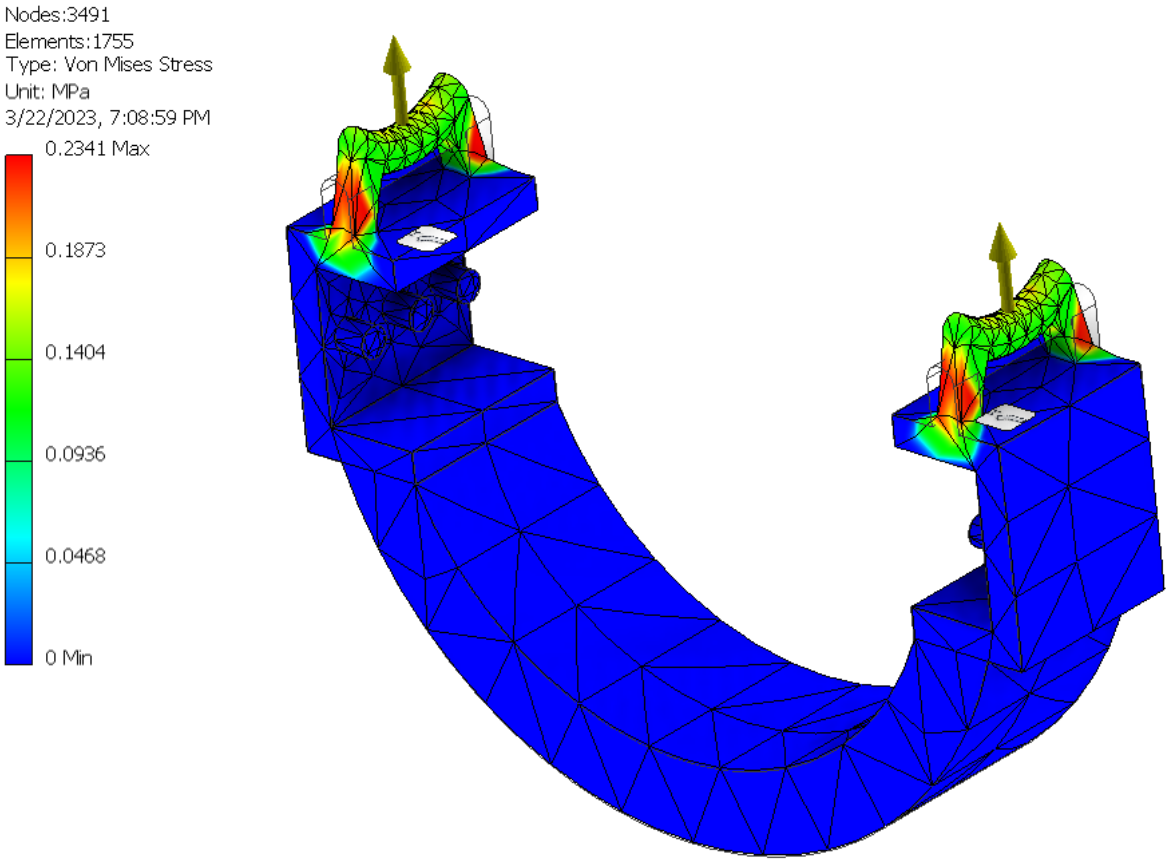

Fig. 19. Stress analysis results of the designed supporter

For the stress simulation, the plane that is in contact with the frame is selected as a fixed point, and forces are added at the tape fastener points. The force was calculated for the 4.47 Nm torque at the nearest fixing point 35 mm from the rotational axis resulting in 127.7 N. Results show that the maximum Von Misses Stress is 0.23 MPa and the stresses are concentrated near the fixing points. The construction is selected to be thick as it will have to support the stress every time the patient is fastening the tape fasteners meaning it will have repetitive overloads.

Additionally, all the supporters have an option to fix in a range of places for more comfortable and individual experience for every patient (see fig. 20.).

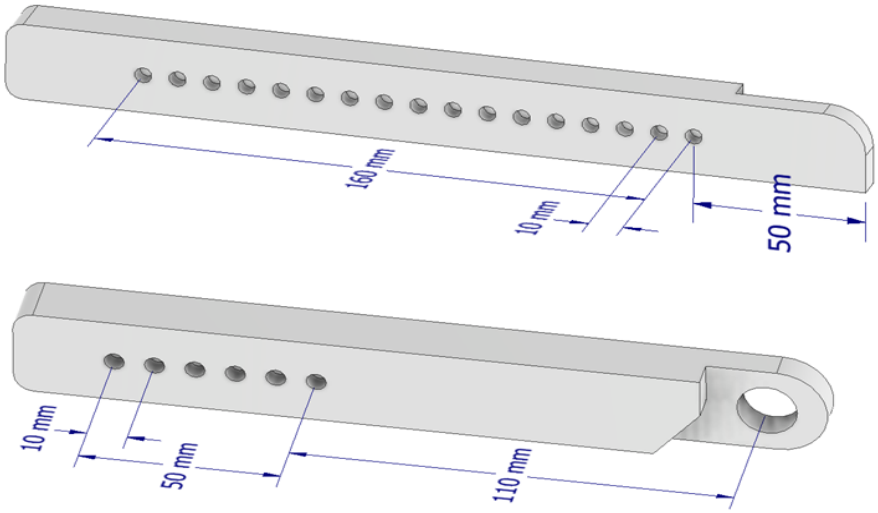

Fig. 20. Mounting options for the supporters on the frame

2.3.4. Maximum and minimum rotational angle restrain on the frame parts

As mentioned in chapter 2, the wearable assistance rehabilitation robot has rotation limitations as the maximum bend angle of the elbow joint is 180 deg. and the minimum angle is 50 deg. It is very important to ensure that the wearable assistance rehabilitation robot would not exceed these limitations as this could harm the person that is performing rehabilitation exercises. In order to limit the rotational angles, custom parts on the end of the frame pieces were designed as shown in fig. 21.

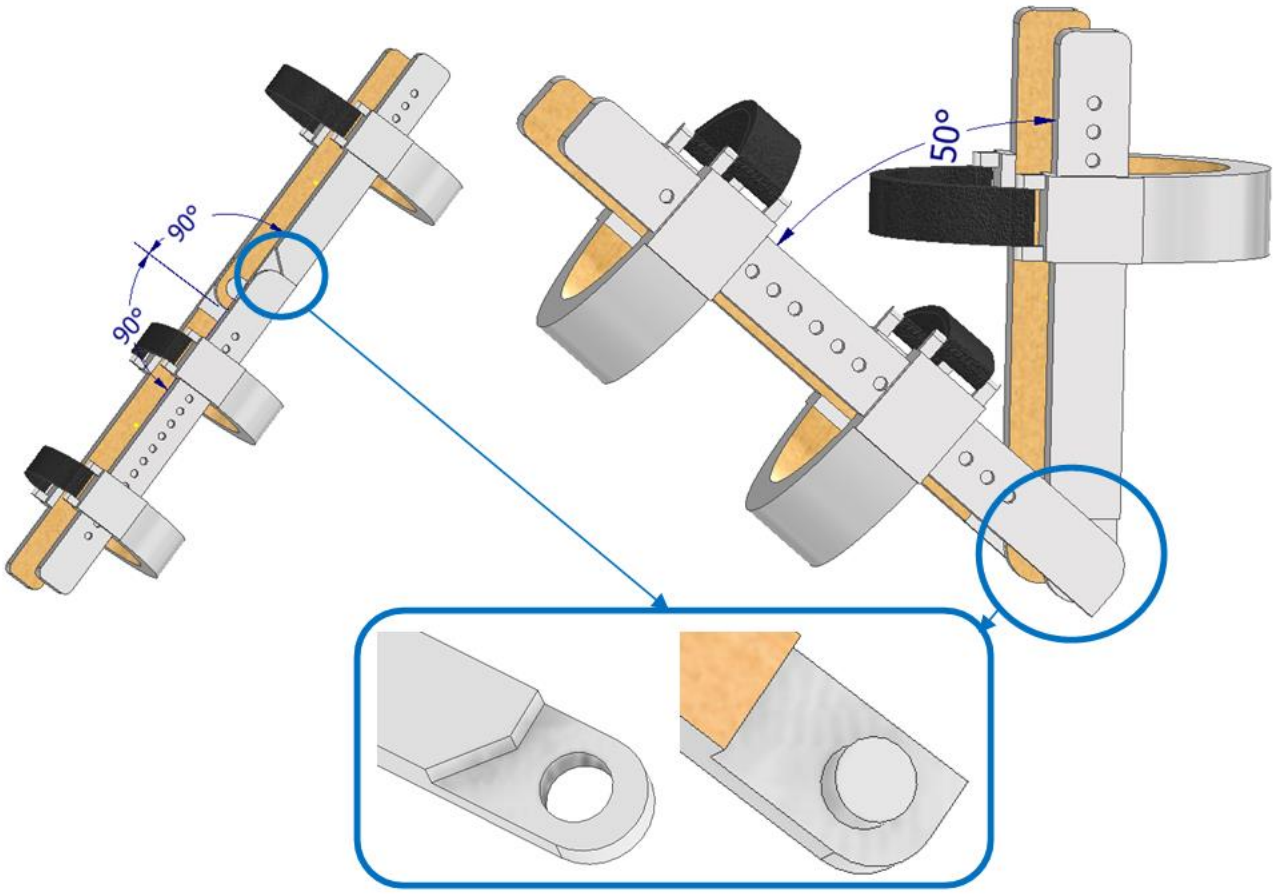

Fig. 21. Rotational angle limitation construction for the wearable assistance rehabilitation robot

As can be seen in fig. 21. the end of frame parts are designed to collide with each other thus preventing the frame to bend more than it is expected. This design will ensure safety of the person while performing the rehabilitation training.

2.4. Material selection research

In order for the frame of wearable assistance rehabilitation robot to be functional and withstand the loads during rehabilitation training while as well being lightweight the most appropriate material has to be selected. The most common materials used by other researchers for the similar frames are usually steel, aluminium or PLA plastic. Steel is known for its hardness, toughness, high tensile strength and machinability. Aluminium on the other hand has low density, great thermal conductivity, excellent corrosion resistance and can be casted or machined easily. PLA plastic has weaker properties but strikes the balance between the impact resistance, rigidity, tensile strength and low density. Table 6. depicts the materials and their properties for the research.

Table 6. Selected materials and their properties

	Steel	Aluminium	PLA plastic
Young's modulus	200 GPa	68.9 GPa	2.91 GPa
Poisson's ratio	0.29	0.33	0.35
Shear modulus	79.7 GPa	25.9 GPa	3500 MPa
Density	7.97 g/cm^3	2.71 g/cm^3	1.29 g/cm^3
Yield strength	350 MPa	275 MPa	38 MPa
Tensile strength	420 MPa	310 MPa	47.2 MPa

The research was made in Autodesk Inventor Professional 2023 stress analysis environment. All frame parts were simulated with loads each time selecting different material from table 6. The results of minimum safety factor of each part with different materials can be seen in Table 7.

Table 7. Minimum safety factor of frame parts with different materials

	Steel	Aluminium	PLA plastic
Upper arm frame part	39	31	4.18
Forearm frame part	36	25	3.37
Upper arm and forearm supporter	1750	1375	165

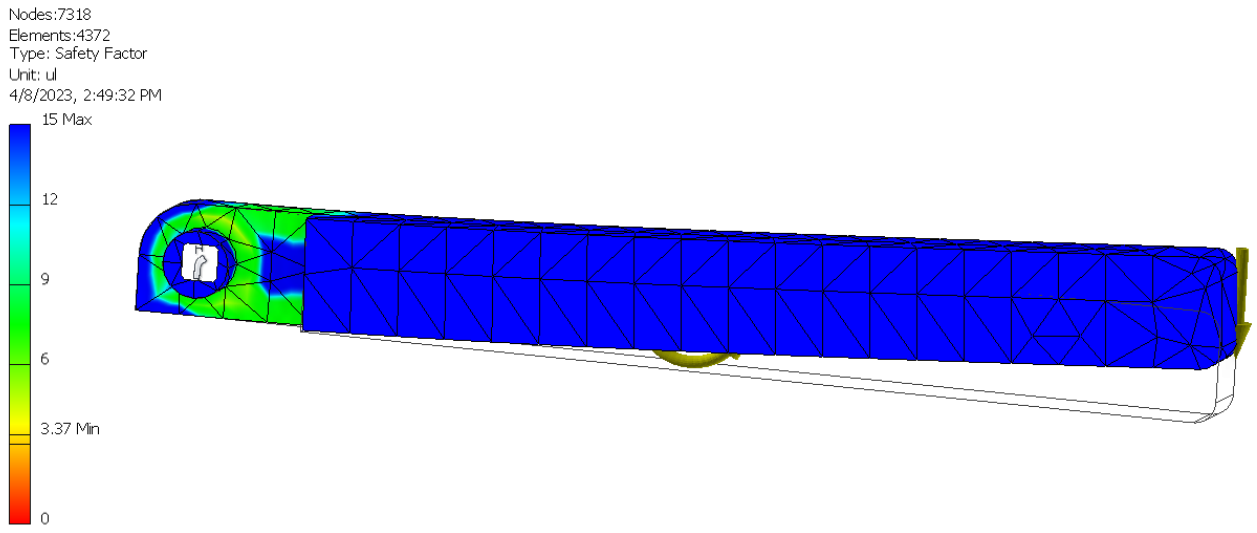

Fig. 22. Minimum safety factor analysis of forearm frame part made from PLA plastic

From Table 7. can be seen that the strongest part is the upper arm and forearm supporter while the weakest part the forearm supporter (see fig. 22). PLA plastic has the lowest minimum safety factors the minimum being 3.37 for the forearm frame part.

What is more, the research of maximum displacements was carried. It had the same principle as the last one. By changing the materials from Table 6. all the parts were simulated with the loads. The results can be seen in Table 8.

Table 8. Maximum displacements of frame parts with different materials

	Steel	**Aluminium**	**PLA plastic**
Upper arm frame part	0.02 mm	0.06 mm	1.37 mm
Forearm frame part	0.03 mm	0.09 mm	2.22 mm
Upper arm and forearm supporter	1.41 x 10^{-5} mm	4.32 x 10^{-5} mm	1.05 x 10^{-3} mm

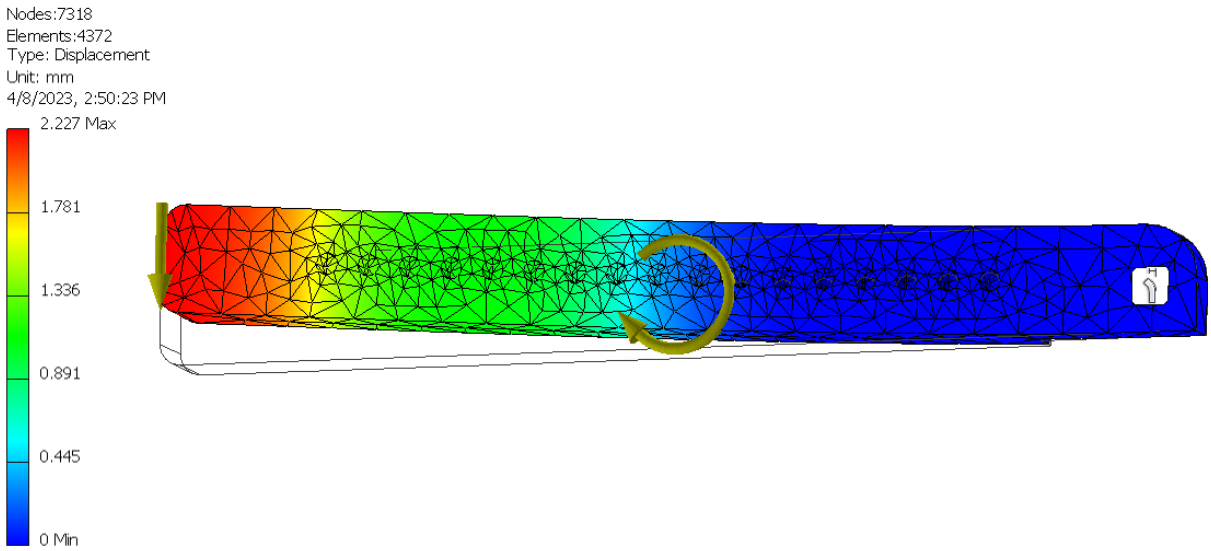

Fig. 23. Maximum displacement analysis of forearm frame part made from PLA plastic

Table 8. depicts that the highest displacement is 2.22 mm on forearm frame part (see fig. 23.) when using ABS plastic. While using steel or aluminium causes minimal displacements.

Lastly, the mass of all the frame parts individually and together was calculated with materials from Table 6. And the results can be seen in Table 9.

Table 9. Mass of frame parts with different materials

	Steel	**Aluminium**	**PLA plastic**
Upper arm frame part	519 g	179 g	85 g
Forearm frame part	671 g	231 g	110 g
Upper arm and forearm supporter	590 g	203 g	97 g
Frame assembly	4.15 kg	1.43 kg	0.68 kg

Results from mass calculation shows that the frame made from steel would be 4.15 kg in mass while produced from PLA plastic would weight 6.1 times less. Meaning PLA plastic can be a valid option as the frame for wearable assistance rehabilitation robot has to be lightweight.

Three materials: steel, aluminium and PLA plastic were chosen as options to produce the frame for wearable assistance rehabilitation robot. After the conducted research it was noticed that the best ratio between strength and weight was achieved when using PLA plastic. The minimum safety

factor when using PLA was noticed in forearm frae part – 2.22 as well as maximum displacement. However the frame that was made from plastic weighted 0.68 kg being 6.1 times lighter than steel and 2.1 times lighter than aluminium. Taking into consideration that 3.37 safety factor is satisfactory, PLA plastic was selected as the main material for the frame of wearable assistance rehabilitation robot.

2.5. Production process analysis of the frame

As the main material for the production of the frame for wearable assistance rehabilitation robot ABS was selected, a 3D printing technology can be used. 3D printing, often called additive manufacturing, creates a product via layering material together, as opposed to conventional or CNC manufacturing procedures that remove material off a solid object and are thus classified as subtractive manufacture. As a result, 3D printing generates minimal wastage of materials, with the exception of the structural supports in the event of complicated forms. There are several methods for 3D printing the object, the most common of which is fused deposition modelling (FDM), see fig. 24, in which fused polymer is deposited layer by layer on a base. As a result, the final product's mechanical qualities are affected by printing factors such as orientation, raster angle, deposition rate, layer thickness, and infill density. Since FDM can manufacture components with very complicated geometries, its ability to endure stress in a variety of applications is critical. Because items are produced by stacking one layer on top of another, the ultimate strength of the pieces is determined by the adhesion among the layers. Such bonding between the layers is mostly determined by the temperatures where each layer contacts with each other during welding. Furthermore, the position of the printed elements through FDM has a significant influence in stress resistance [19-20]. These essential stages are involved in 3D printing. It all begins with a 3D model and this 3D design is next sent into a slicing engine to build a printing toolpath. The component is built according upon the provided toolpath. The next phase is post-processing, which involves removing supporting elements from the manufactured item [21].

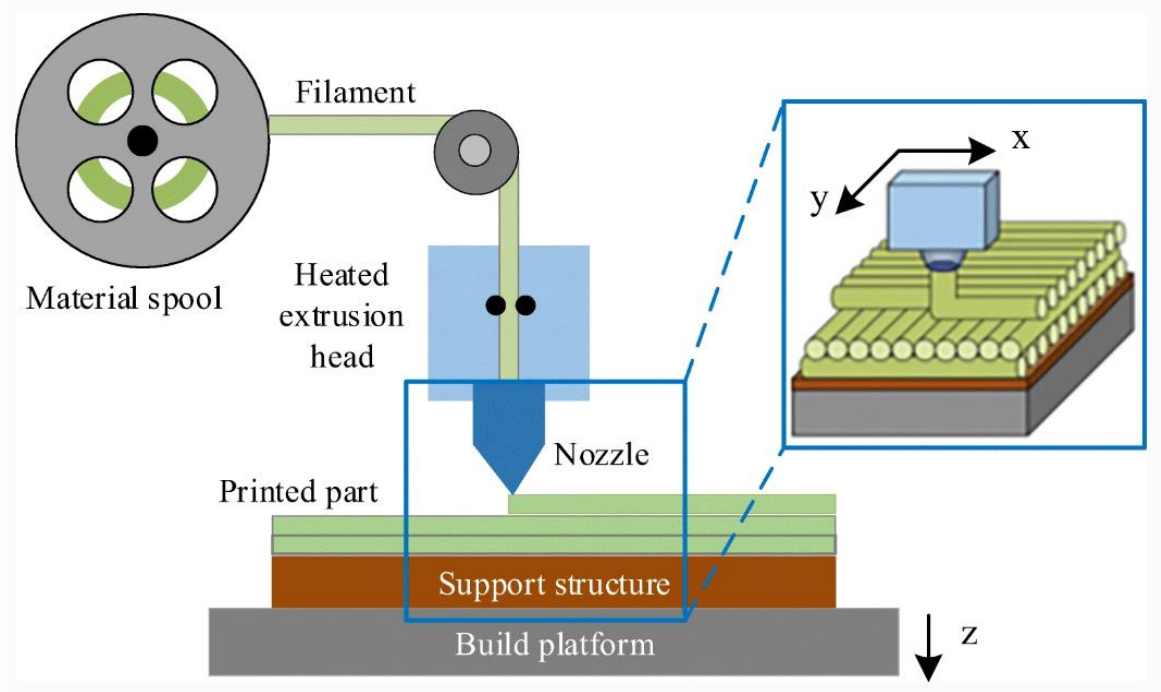

Fig. 24. FDM printing process [21]

In order to prepare for the printing of the frame for wearable assistance rehabilitation robot the designed parts have to be converted into stl type of file in order for the slicing program to process the data. An example of converted upper arm supporter can be seen in fig. 25:

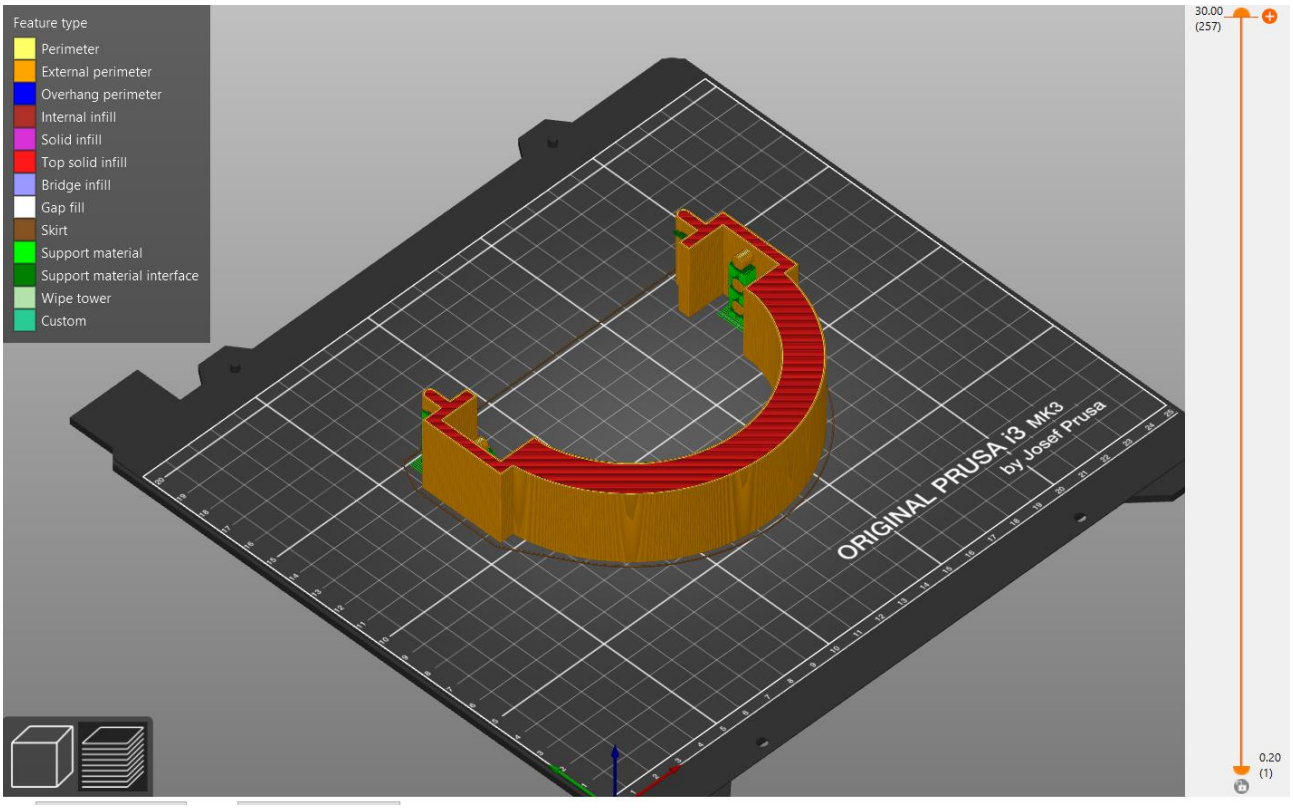

Fig. 25. Sliced upper arm supporter

When the detail is imported into the slicing program, in this case the PrusaSlicer 2.0 was used, the detail then can be seen as how it will be positioned on the printing bed. Then there is an option to change its position, angle or alignment. After that the user has the option to choose from additional settings as the printing settings, filament, printer, support type and the infill. These parameters and options can be seen in fig. 26-27:

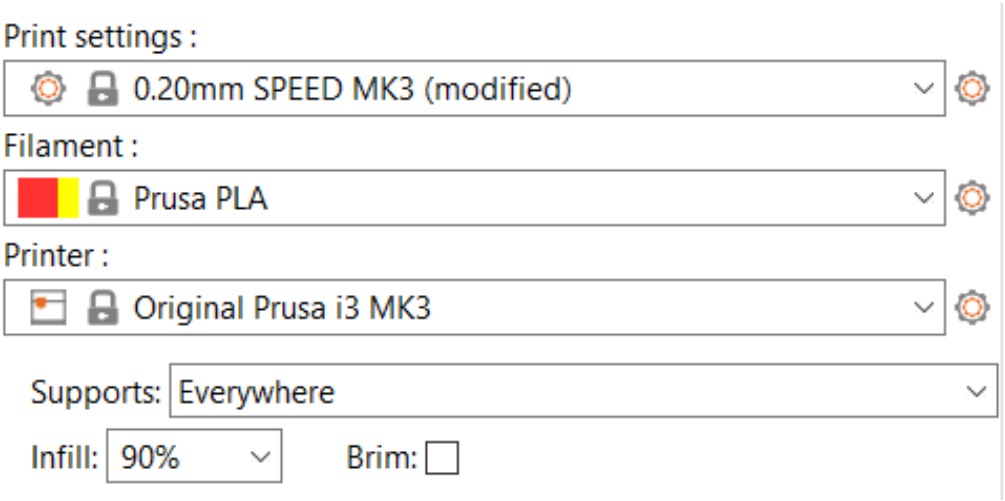

Fig. 26. Print settings of the upper arm supporter

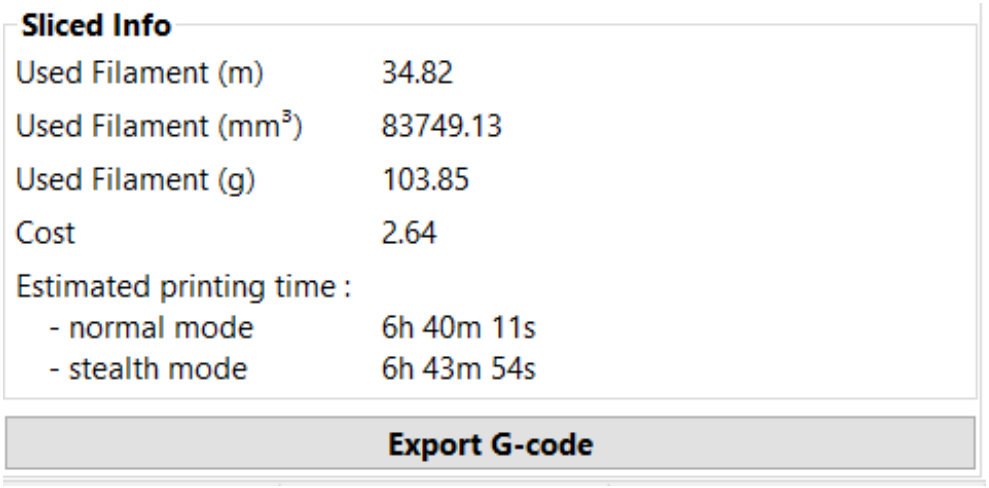

Fig. 27. Sliced information of the upper arm supporter

Fig. 26-27. depicts that the filament for the printing process was selected to be PLA plastic, as discussed in previous chapter. The supports were also selected to be everywhere. That means that all the hanging parts as for example the pins in the upper arm supporter will have a printed support that will allow to print them. Supports are recommended to achieve the best printing results. For this testing the infill was selected to be 90%, however it can be changed and a research should be conducted in order to find the best printing parameters for this specific thesis case. In the sliced info segment the used filament can be seen, as well as the mass of the printed detail. The mass of the printed detail may vary from the simulated in the Autodesk Inventor programme as the infill and support material has the impact on the final mass of the detail. The printing time for the selected part was also calculated to be 6h and 40m. After all the parameters are selected and the sliced results are satisfactory then all the printing information then can be exported to the G-code. The G-code contains instructions and tool path for the 3D printer to perform the printing process as described in the slicing program. Finally, some post processing has to be done after the detail is printed. Removing the support material, grinding out sharp features that are left after printing with the help of sand paper. After little post processing the part is ready to use for the wearable assistance rehabilitation robot.

2.6. Motor and gear mechanism selection

Permanent magnet DC motors are used in various motion-based systems. Because DC motors are simpler to install control systems than AC motors, they are frequently utilized whenever speed, torque, or position must be regulated. Brushed motors as well as brushless motors are the two most prevalent types of DC motors. DC brushed motors, as the name implies, feature brushes that are utilized to commutate the motor and enable it to rotate. Brushless motors use electronic control to substitute mechanical commutation. A brushed or brushless DC motor may be utilized in numerous situations. They work according to the identical concepts of attraction and repulsion that coils and permanent magnets do. Both have benefits as well as drawbacks (see fig. 28) that may result to a preference between the two based on the application's needs [22].

	Brushed DC Motor	Brushless DC Motor
Lifetime	Short (brushes wear out)	Long (no brushes to wear)
Speed and Acceleration	Medium	High
Efficiency	Medium	High
Electrical Noise	Noisy (brush arcing)	Quiet
Acoustic Noise & Torque Ripple	Poor	Medium (trapezoidal) or good (sine)
Cost	Lowest	Medium (added electronics)

Fig. 28. Comparison between brushed and brushes DC motors [22]

Taking into consideration the data from fig. 25. a brushless DC motor was selected for the control of the wearable assistive rehabilitation robot. For this specific application an external rotary, brushless DC motor DFA68M024037-A (see fig. 29.) from the company Nanotec was selected. This motor is a cost effective solution and is shorter than its competitors. Technical data of the motor DFA68M024037-A can be found in Appendix 1.

Fig. 29. Selected brushless DC motor DFA68M024037-A [23]

In order to achieve the required maximum 4.47 Nm torque a gearbox has to be selected for the brushless DC motor. A GP56-S2-20-SR (see fig. 30.) high torque planetary gearbox from Nanotec was implemented. Planetary gearboxes have a very high torque and efficiency that is why it is a great option for the wearable assistive rehabilitation robot. Due to the low backlash this gearbox is perfectly suited for the applications that demand exact positioning. Technical data of the planetary gearbox GP56-S2-20-SR can be found in Appendix 2.

Fig. 30. Selected planetary gearbox GP56-S2-20-SR [23]

The selected brushless DC motor as well as the planetary gearbox can be easily connected and the combined characteristics can be seen in fig. 31:

Size	68 mm
Weight	1.3 kg
Rated Speed	185 rpm
Rated Torque	5.2 Nm

Fig. 31. Parameters of the selected motor and gearbox combination [23]

As can be seen from fig. 31. the rated torque of the selected brushless DC motor and planetary gearbox is 5.2 Nm that is satisfactory as the highest calculated torque that is needed for the wearable assistance rehabilitation robot is 4.47 Nm. The torque and RPM will be further controlled with the help of the controller in order to achieve optimal rehabilitation exercise parameters.

The general assembly of the wearable assistance rehabilitation robot with the frame and implemented motor and gearbox as well as the patient for scale can be seen in the fig. 32:

Fig. 32. General view of the wearable assistance rehabilitation robot on the patient

Fig. 32. depicts the assembly of wearable assistance rehabilitation robot that the patient is using. The motor and gear mechanism will be mounted on the frame with the help of the key on the gearbox shaft, this will ensure rotary motion transfer. The motor and gearbox assembly will be also held in place with the help of the cover box. It will store the motor and gear as well as electrical part of the wearable assistance rehabilitation robot. The cover box will be mounted to the frame with the help of bolts and nuts.

2.7. Results of the robot frame design

The frame for the wearable assistance rehabilitation robot was designed using Autodesk Inventor Professional 2023 software. Using the stress analysis environment the loads were added and maximum Von Misses stress of 11.27 MPa was calculated. Material research was conducted between steel, aluminium and ABS plastic in order to select the best applicable material for the production of the frame. With the satisfactory minimum safety factory of 1.77, maximum deformation of 2.92 mm and total weight of 0.56 kg ABS plastic was selected. The production process analysis was made and 3D printing FDM method was analysed as a valid production method for the frame. Lastly, brushless DC motor DFA68M024037-A with a combination of planetary gearbox GP56-S2-20-SR was selected. Combined rated torque of the selected motor and gearbox assembly was 5.2 Nm and the total mass of 1.3 kg. A general preview of the wearable assistance rehabilitation robot with the patient was presented and the assembly was discussed.

2.8. Automation of wearable assistance rehabilitation robot

In order for the wearable assistance rehabilitation robot to be automated, it needs sensors that would send a feedback data and a controller to analyze the feedback and operate the motor. A control method and algorithm should also be discussed in order to achieve the best rehabilitation results.

2.9. Inductive proximity sensors

An inductive proximity sensor (see fig. 33.) will be used in order to determine the maximum and minimum positions of the wearable assistance rehabilitation robot. As discussed in the modelling chapter, the frame will have restriction to not bend over the limits. An inductive proximity sensor will be inserted in the frame and the metal pieces will be embedded in the opposing frame part (see fig. 34), so that once the frame is bent to the limit, the sensor will send a signal to the control unit that the robot has reached the maximum distance and it should be stopped.

Fig. 33. Selected inductive proximity sensor Contridex DW-AD-711-04 [24]

A Contridex DW-AD-711-04 inductive proximity sensor was selected as it is small in dimensions and has a 4mm diameter body.

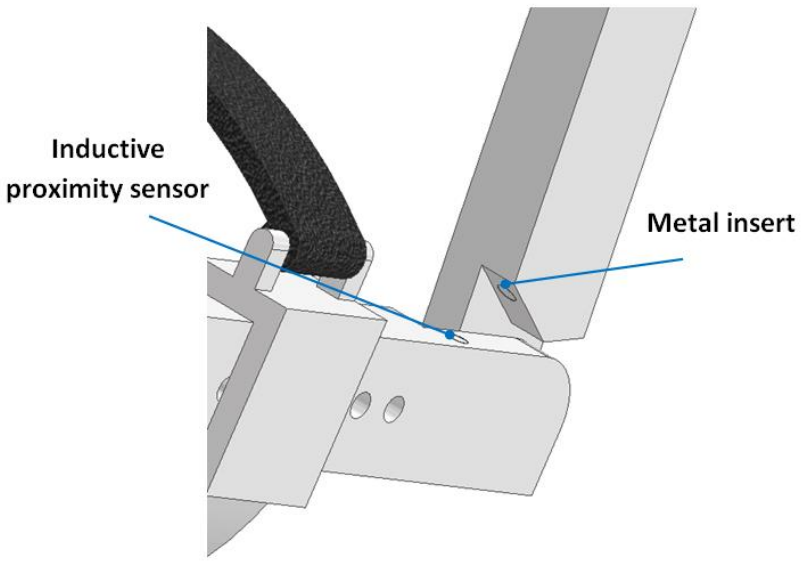

Fig. 34. Implementation of inductive proximity sensor

The usage of inductive proximity sensors will ensure safe exploitation of the wearable assistance rehabilitation robot by providing feedback for the control unit and avoiding collisions and exceeding of maximum and minimum bending angles.

2.10. Remote controller

As the wearable assistance rehabilitation robot will be able to rotate around the elbow joint, change the torque and speed, the user has to have an option to control these parameters while performing rehabilitation training. That is why the remote controller was designed (see fig. 35.). This remote controller will have basic options as power, speed and movement control.

Fig. 35. Designed remote controller for the wearable assistance rehabilitation robot

The patient will be holding the remote controller in the hand while performing the training exercises. By controlling the power, the person will be able to increase the torque of the robot if one needs more support in bending the upper limb and decrease the torque if the patients feels like the amount of assistance is unnecessary. The speed option will let the patient to control the speed in which the robot is bending, in other words, angular speed. And finally the patient will be controlling the movement of the robot by pressing to increase the bending angle and decrease it. The remote controller will ensure comfortable experience and control over the exercise process. Lastly, to ensure the safety of the patient in case of the remote controller falling of the hands and accidentally pushing the control buttons a kill switch bracelet will be implemented (see fig. 36.).

Fig. 36. Kill switch bracelet [25]

The kill switch bracelet will be directly connected to the remote controller and in case of the remote controller falling off the hand it will instantly stop the wearable assistance rehabilitation robot preventing any unwanted button presses after the controller has fallen on the ground. This is a necessary mean of safety for the wearer.

2.11. Motor controller

For the control of the motor a motor controller has to be selected. The motor controller has to have speed and torque control options as well as rotate and break the motor on demand. For this case a motor controller C5-E-2-09 from Nanotec (see fig. 37.) was selected. This controller is compatible with the selected brushless DC motor and has several useful functions that will aid in the control of the motor.

Fig. 37. Selected motor controller C5-E-2-09 [26]

The selected motor controller has velocity and torque control options, homing option and motor overload protection as well as automatic brake control. The controller has 10 I/O ports as well as micro USB connection. It can be programmed with the specific software provided by the supplier.

2.12. Battery

In order for the wearable assistance rehabilitation robot to be comfortable and used anywhere on demand, a battery pack will be integrated inside the robot. Meaning the robot will not need any external power supplies and will be extremely flexible to use in contradiction to the reviewed competitors that are tied to the external power supplies meaning they can be used only at the specific location. For this project a 24V 3Ah Lithium ion battery pack (see fig. 38.) was selected. Lithium ion batteries are well known for their long cycle life and this option is great for the wearable assistance rehabilitation robot.

Fig. 38. 24V 3Ah Lithium ion battery pack DNK-LTB2430 [27]

In order to calculate the working time of fully charged wearable assistance rehabilitation robot the following calculation is used:

$$t = \frac{C_b}{I_m + I_i + I_i} = \frac{3}{5.6 + 0.2 + 0.2} = 0.5\ h$$

Where: t is the working time of the fully charged robot (h), C_b is the charge capacity of the battery (Ah), I_m is the rated current of the motor (A), I_i is the rated current of proximity sensor (A).

As can be seen from calculations, that the maximum working time of the fully charged robot is 0.5 hours, however this is taken into account that the motor is running at the full capacity which will not happen when exercising, meaning the average training time with the fully charged wearable assistance rehabilitation robot will be about 1 - 1.5h.

2.13. General electrical diagram

The general electrical diagram can be seen in fig. 39. Both proximity sensors are connected to the +10V supply with the R1 and R2 resistors that are 24kΩ each. They go into motor controller X3 input/output block into pins 2 and 3 – digital inputs. The move "+" and move "–" buttons are also connected to the X3 input/output block and go into pins 4 and 5 – digital inputs. The power and speed potentiometers are connected to the analog inputs 7 and 8 in the X3 block. The kill switch is connected in a way that if it is cut off from the circuit the other buttons will not function as a safety measure. All inputs are connected on the same ground that is in X3 input/output module pin 12. The motor is connected to the X5 block that is assigned for motor connection and the encoder of the motor is connected to the X2 block that is assigned for the encoder/hall sensor. The 24V battery itself is plugged into the X6 block that is assigned as the voltage supply. The finalized general scheme will ensure the correct and comfortable control of the wearable assistance rehabilitation robot. The user will have a full control over the parameters and movement of the robot as well as will be protected from any accidental inputs if the controller falls of the hands when the kill switch is active. In this way a user friendly control interface of the assistance rehabilitation robot is implemented.

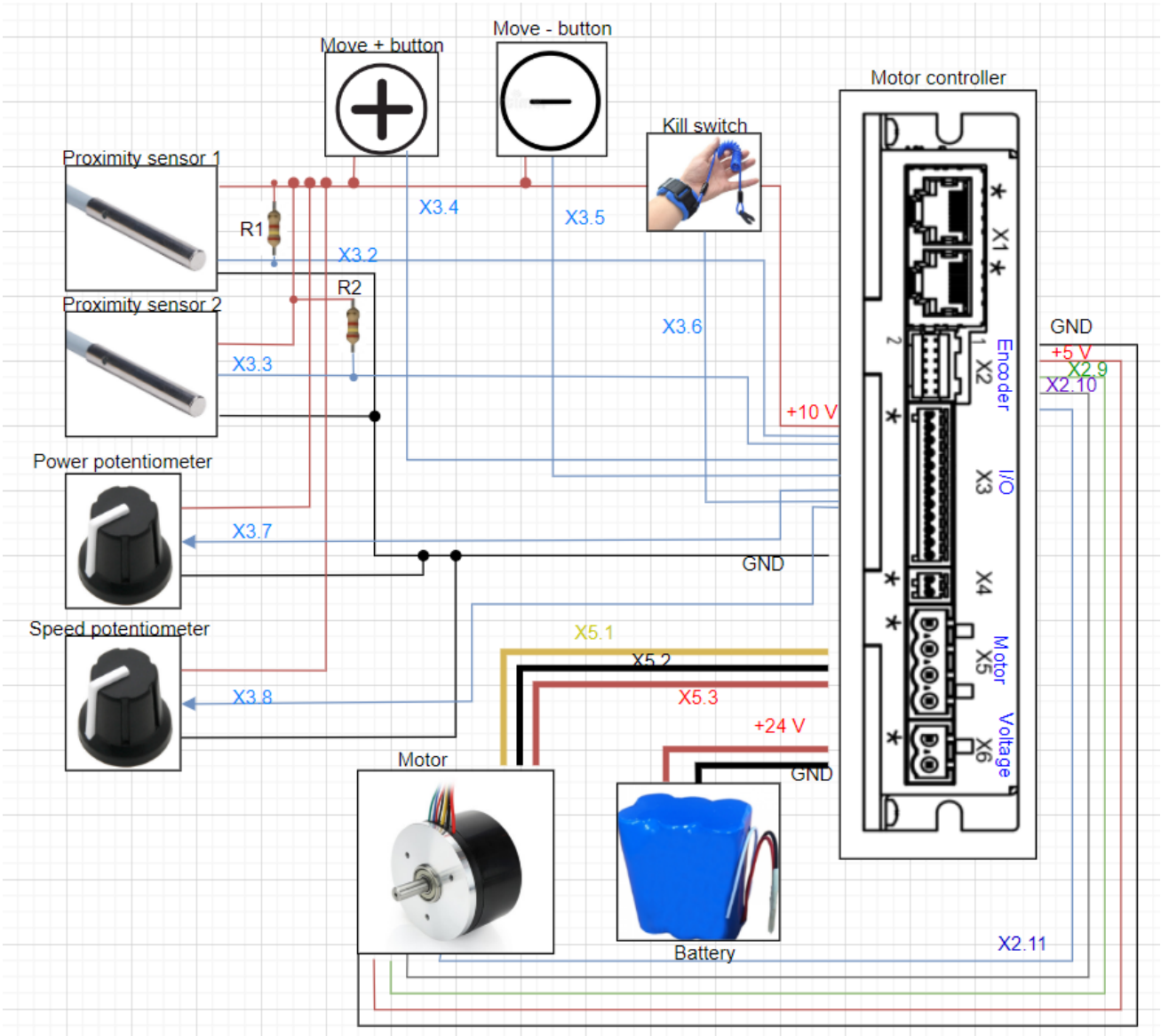

Fig. 39. General electrical diagram

2.14. Control algorithm

The control algorithm that can be seen in fig. 40. working principle is as follows: first of all the wearable assistance rehabilitation robot is turned on. Afterwards, the algorithms checks if the kill switch is not active, and if not its starts to wait for the input from the remote controller. If the power or speed potentiometers are moved, the algorithm checks if the maximum or minimum value were not exceeded and then depending on the answer either will allow to make changes or will not proceed to go beyond limits. When the move button is pushed the algorithm checks if the inductive proximity sensors are not active and will act upon the command of the user. When the angle reaches the maximum or minimum values the sensors stop the movement. If the kill switch is activated at any time, the wearable rehabilitation robot is turned off.

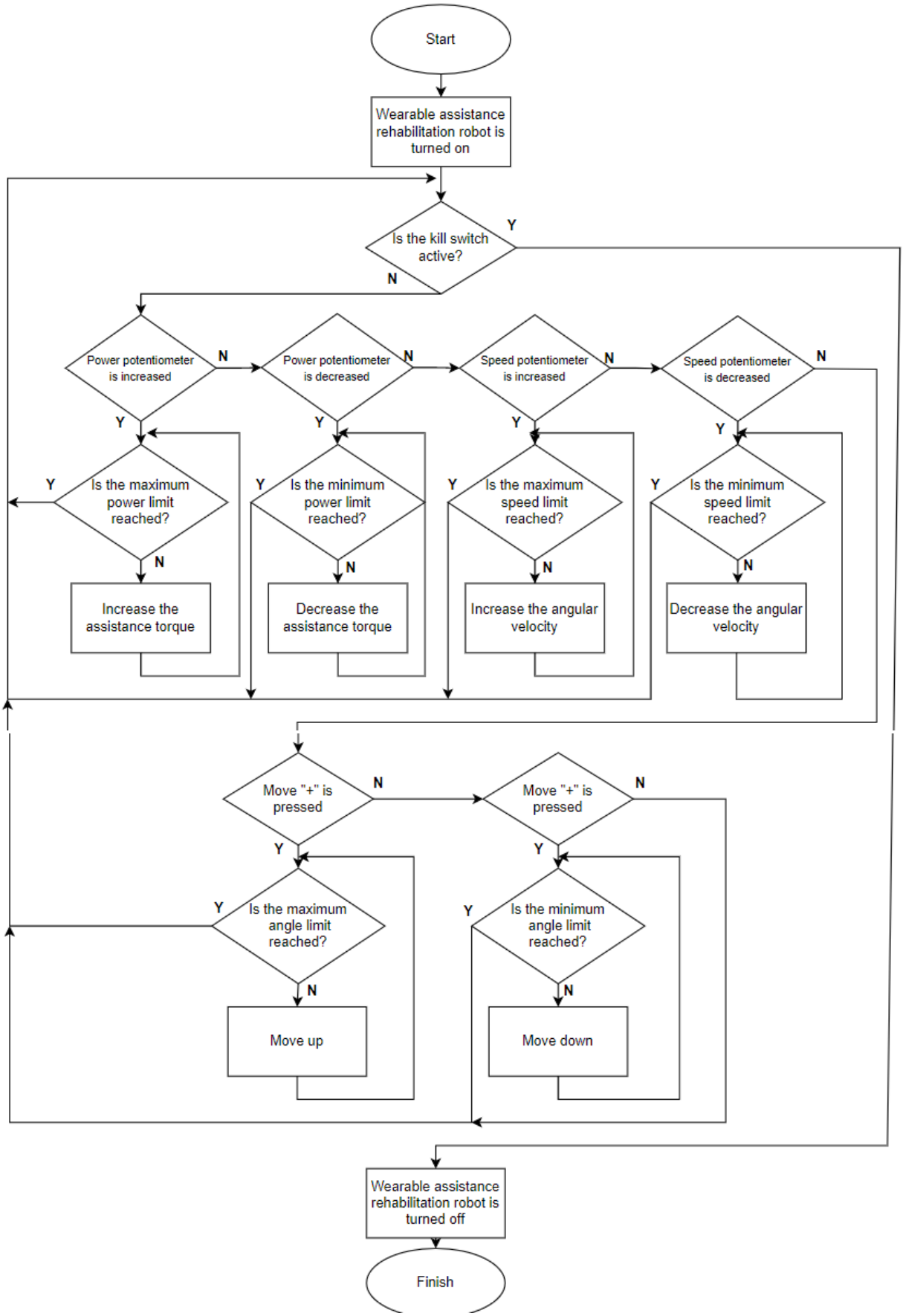

Fig. 40. Control algorithm for the wearable assistance rehabilitation robot

2.15. Control box assembly

All the required electrical components for the wearable assistance rehabilitation robot will be stored in single control box that will be attached to the robot frame. In this case the robot will be wearable and easily transportable without any additional external components. The general view of the assembly with all the main parts can be seen in fig. 41.

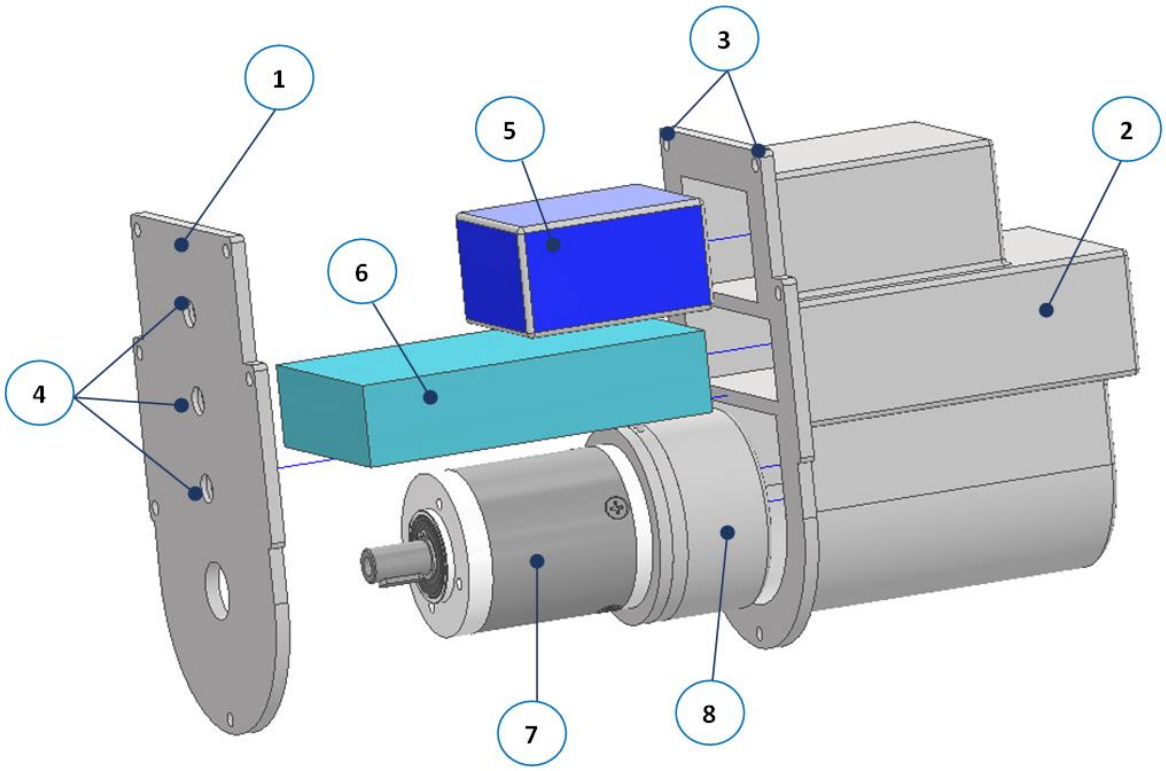

1 – Control box cover; 2 – Control box; 3 – Fixing points of control box and cover; 4 – Fixing points of cover and robot frame; 5 – Battery; 6 – Motor controller; 7 – Reduction gear; 8 – Motor;

Fig. 41. Assembly of the control box for wearable assistance rehabilitation robot

As depicted in fig. 41. all the components will be fitted in the control box. The control box itself will be closed with the help of control box cover and 6 M5 screws. The control box will be attached to the robot frame with 3 flat head M10 screws that will be fixed with the control box cover. Battery, motor control unit and the motor with the gear will have separate sections in the control box. All these sections have a communication holes at the end so that all the wires could be connected easily. The control box and control box cover will be also 3D printed from PLA plastic. In this way, the frame will be lightweight and easy to produce as the robot frame will be printed from the same material. The man advantage of this assembly is that it will allow the patient to wear the rehabilitation device anywhere on demand and transport it without difficulties. The reviewed analogs all have a non portable control box that needs to be held stationary thus limitating the options and possibilities for the person to perform rehabilitation training. The designed compact control box will eliminate this problem and the person using the wearable assistance rehabilitation robot will be able to do the tasks for rehabilitation anywhere on demand.

2.16. Alternative control method using a wearable tactile sensor array

It is important to mention that an alternative control method for the wearable assistance rehabilitation robot can be implemented. Scientists from China have developed a wearable wrist gesture recognition band. The Flexible Epidermal Tactile Sensor Array (FETSA) is utilized to measure the physical deformation of the sensor as a result of wrist movement [28]. The sensor collects data in the form of a change in electrical resistance caused by muscle action. An array of 16 sensors is utilized for the wearable wrist band (see fig. 42.).

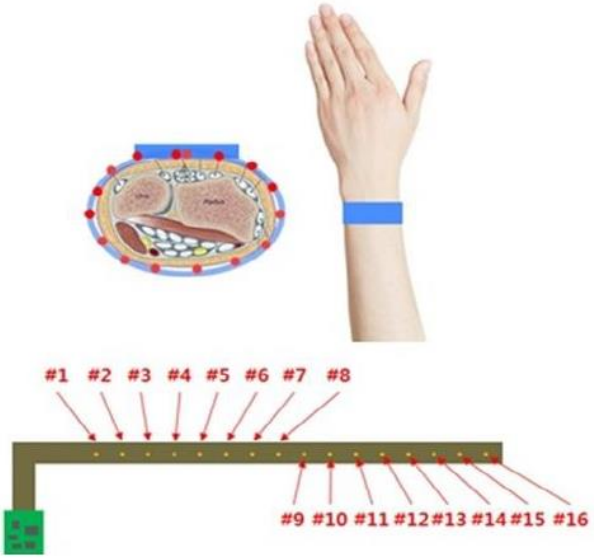

Fig. 42. Sensor array of wearable wrist gesture recognition band [28]

The FETSA comprises of a strain gauge whose resistance can alter depending on the motion of the wrist on a flexible substrate in order to identify the deformation of the sensor in a reliable manner. As a result, the FETSA detects the change in resistance caused by the relaxation and contraction of wrist muscles [28]. The gesture recognition wrist band can detect several gestures that would allow to control wearable assistance rehabilitation robot. Several gestures and their uses are described in fig. 43.

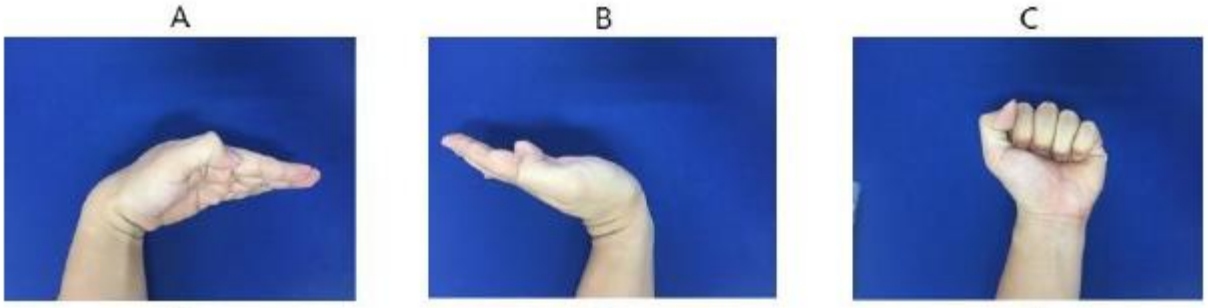

Fig. 43. Gestures for wearable assistance rehabilitation robot control: a) – move up, b) – move down, c) – stop [28]

Implementing the wearable wrist gesture recognition band could improve and ease the control of the wearable assistance rehabilitation robot. However, this is just a reviewed alternative as implementation would require further compatibility research.

2.17. Designed wearable assistance rehabilitation robot

The final design of the wearable assistance rehabilitation robot can be seen in Fig. 44. The robot consists of the main frame – upper arm and forearm frame parts and supporters as well as tape fasteners to ensure good fixture on the arm. All of the control components are stored inside the control box that is fixed to the main frame with the help of 3 flat head M10 bolts. The control box stores the motor and the gear itself, the motor controller that is ensures the control of the motor during the rehabilitation trainings and a lithium ion battery for about 1 to 1.5 hours of usage between charges.

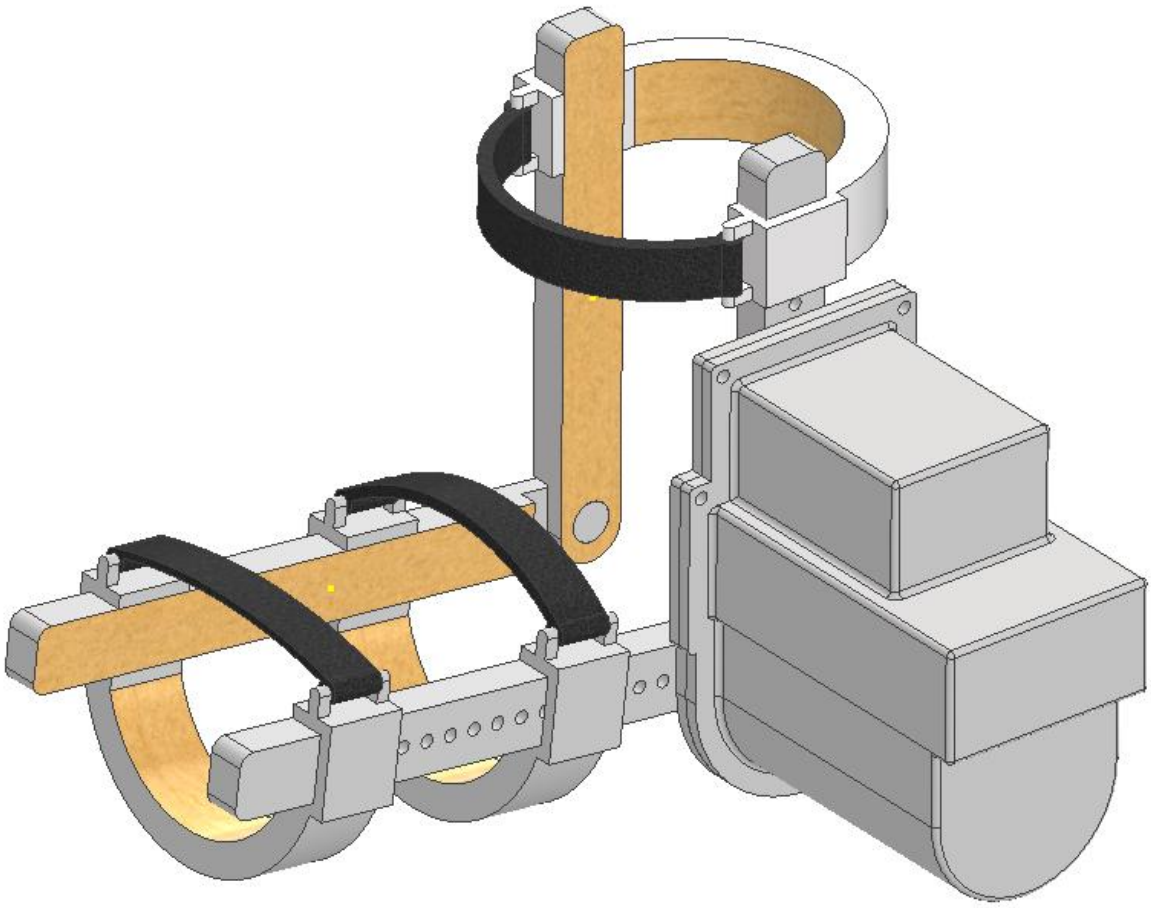

Fig. 44. Designed wearable assistance rehabilitation robot

The wearable assistance rehabilitation robot can be easily worn by the patient anywhere and does not require any additional external elements apart from the remote controller that is used to adjust power, speed of the robot as well as control it to bend up or down. The robot frame itself is designed to limit the movement of the elbow joint in the range of 50-180 degrees in order to avoid injures. Inductive proximity sensors are also installed so that the robot would know when it reaches the maximum or minimum angles. Finally the kill switch bracelet is worn during the training in order to protect the patient if any accidental remote controller buttons are pressed when the remote is lost. All the components mass and costs are written in table 10. Note that for the 3D printed parts only the cost of the material was taken into account when calculating the cost.

Table 10. Component mass and cost of wearable assistance rehabilitation robot

Part	Mass, kg	Cost, Eur
Main Frame	0.68	15
Control box	0.51	11
Battery	0.28	80
Motor	0.47	107
Reduction gear	0.79	144
Motor controller	0.27	275
Additional fixing elements	0.1	10
Total	**3.1**	**382**

As can be seen from the table 10, the total mass of the wearable assistance rehabilitation robot is 3.1 kg. The heaviest being the reduction gear at 0.79 kg. A lot of weight was saved as the PLA plastic was chosen for the main frame, as for example the frame from steel would have weighted 4.15 kg as from research done in material selection chapter. The total cost of the wearable assistance rehabilitation robot is calculated to be 382 Eur. This cost is preliminary and is not affected by the printing expenses and engineering time.

2.18. Summary

In this chapter an automation components for the wearable assistance rehabilitation robot were selected. The inductive proximity sensors were chosen in order to determine the maximum and minimum bending angles for the robot and send the feedback data to the controller. The motor controller was selected specifically to be compatible with the selected motor. The controller is able to change the torque, speed of the motor as well as it can be programmed in order to performed the required operations. The remote controller was suggested in order for the patient to have full control over the robots speed, power and movement. A safety kill switch bracelet was chosen to avoid any unintentional remote control actions in case of an accident. Finally the control algorithm was made for the motor controller as well as a general electrical diagram. An alternative option of the control method was also suggested. A tactile sensor array wrist band could be implemented, however it would require further research and testing. Lastly a control box was designed to store all the automation components as well as the 24V lithium ion battery with a life time of 1-1.5 hours of uninterrupted exercising. The total weight of the designed wearable assistance rehabilitation robot is 3.1 kg and the preliminary cost without the expenses of 3D printing and engineering work was calculated to be 382 Eur. An affordable, automated and wearable robot was designed.

3. Research of mechanical properties of 3D printed specimens from PLA for the wearable assistance rehabilitation robot frame.

As discussed in chapter 3, the frame for wearable assistance rehabilitation robot will be produced using a 3D printing FDM technology from PLA plastic. In order to understand properties of 3D printed PLA plastic, a research has to be conducted where 3D printed specimens would be tested in the laboratory for their exact mechanical properties, as the simulations in Autodesk Inventor can only be considered as a guideline because the Inventor stress analysis simulation takes the whole part to be isotropic, and 3D printed plastic has slightly different characteristics. In this research, 5 types of different specimens were tested in 3 point bending test. The types differ in infill ratio and internal printing geometry. A 3 point bending test was selected as it would most accurately depict the required properties of 3D printed plastic for the specific application as the robot frame parts are bended when they come in contact.

3.1. Preparation and printing

For the bending test a 3 point bending test standard ISO:178 for plastics was chosen. A specimen of 80x10x4 mm was designed as described n the standard (see fig. 45). The specimen was designed using Autodesk Fusion 360 environment.

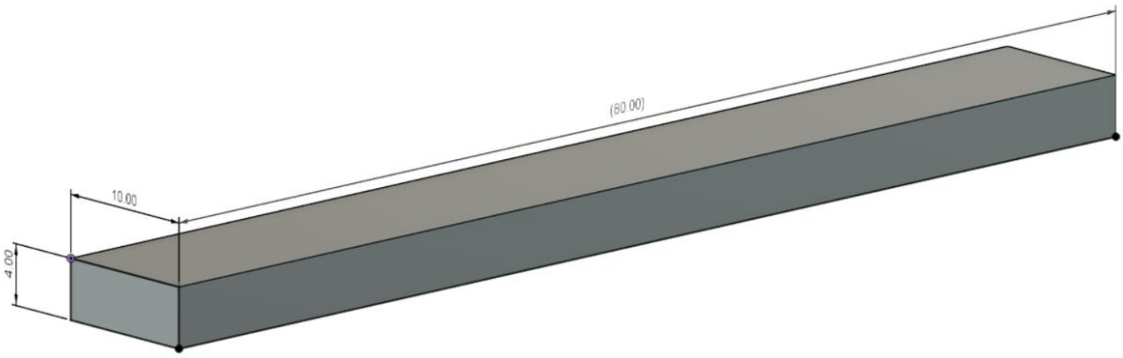

Fig. 45. Specimen for 3D printing

After the design, the specimen was transferred to a slicing software IdeaMaker 4.2.3. First of all general printing parameters were selected for all specimens:

Table 11. General printing parameters for all specimens

Layer height	0.2 mm
Shells	3
Extrusion width	0.6 mm
Supports	None
Heated bed temperature	60 ^{o}C
Primary extruder temperature	210 ^{o}C
Default printing speed	100 mm/s

When the general parameters were chosen, 5 different types of specimens were designed with different infill types and printing pattern geometry:

Table 12. Slicing parameters of different types of specimens

	Type 1	Type 2	Type 3	Type 4	Type 5
Infill density, %	100	100	100	60	60
Infill pattern type	Solid	Solid	Solid	Gyroid	Cubic
Solid fill pattern type	Lines	Rectilinear	Concentric	Lines (shells)	Lines (shells)

As can be seen from table 12, first three types were chosen to be solid with 100% infill and different solid infill pattern types while the rest were selected to be 60% infill and have different infill pattern types in order to determine what impact does not only different infill but different infill geometry have on the mechanical properties of the 3D specimens. The sliced specimens of different types can be seen in fig 46.

Fig. 46. Sliced specimens of different types

For the PLA plastic a HP-PLA plastic from Creality was used. Specifications of the selected plastic can be found in table 13.

Table 13. Specifications of the selected PLA plastic [29]

Product name	HP-PLA
Supplier	Creality
Printing temperature	210-240 ^{o}C
Filament diameter	1.75 mm
Tensile strength	60 MPa

The 3D printer that was used for printing the specimens was Creality CR-10S (see fig. 47), more technical information about the 3D printer can be found in appendix 3. The 3D printer was placed in a specific heat maintaining box with the humidity of 15% and internal temperature of 26.7 ^{o}C.

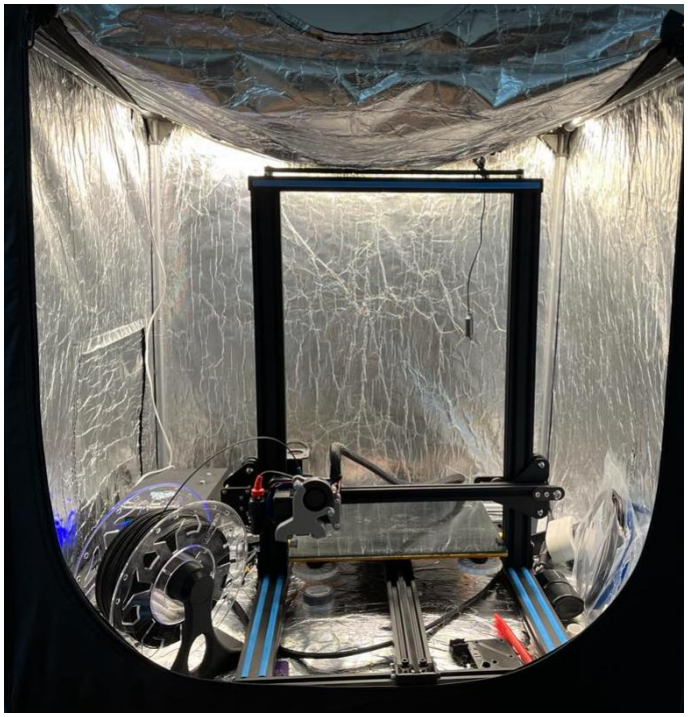

Fig. 47. Creality CR-10S printer

For the accuracy of the results 3 pieces of specimens were printed for each type. The printing process was done in two prints as the printing bed could not facilitate all specimens at once. The printing process parameters are described in table 14.

Table 14. Printing process parameters

	First print	Second print
Printing time	1 h 10 min	55 min
Used filament, g	31.7	23.6
Used filament, m	10.63	7.91

Printing process went without any issues and printed specimens were ready to be tested.

3.2. 3 point bending test and results

A 3 point bending test was conducted in the KTU University's laboratory with a help of qualified staff member. A testing machine Tinius Olsen H10KT (see fig. 48) was used for the experiment.

Table 15. Technical specification of Tinius Olsen H10KT testing machine [30]

Working temperature	-70 ºC – 300 ºC
Maximum load	10 kN
Sensor	10kN
Testing speed	0.001 – 300 mm/min

Fig. 48 Tinius Olsen testing machine

Specific parameters and testing equipment was selected for this experiment.

Table 16. Testing parameters

Test speed	5 mm/min
Preload	0 N
Distance between supports	63 mm
Support radius	5 mm

After the testing parameters were written to the computer and selected supports were placed the specimens were tested separately by type.

3.2.1. Results of specimen type 1

Specimen type 1 was tested and the results can be seen in table 17 and fig. 49:

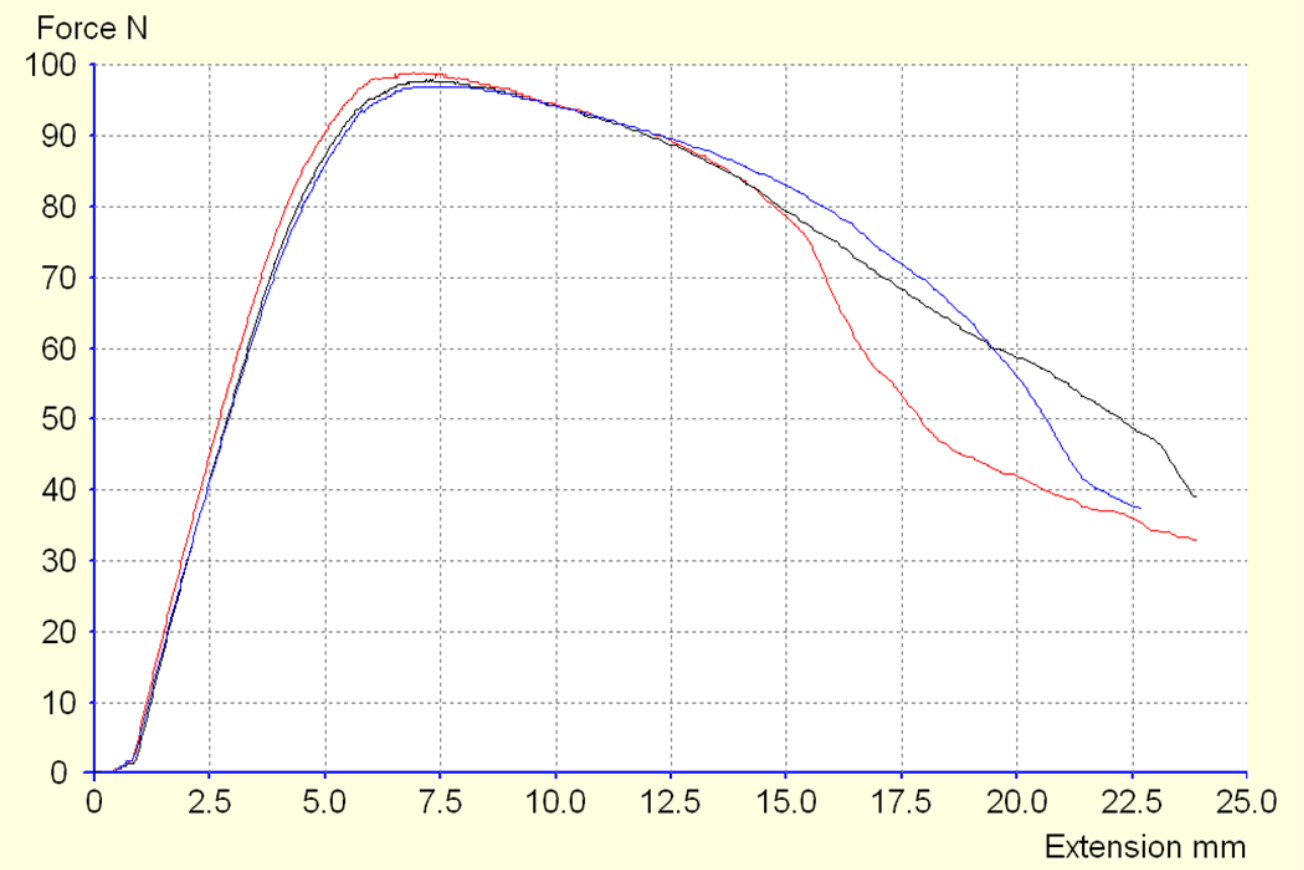

Fig. 49. 3 point bending test results of specimen type 1

Figure 49 depicts the force and displacement relationship of all three type 1 specimens. Maximum values of each specimen can be seen in table 17.

Table 17. Results of specimen type 1

Specimen	Max force, N	Displacement at max, %	Elongation,%
1	99	172.5	598
2	98	180	598
3	97	172.5	568
Mean	98	175	588
Std. Dev.	1	4.33	17.32

As can be seen from the results the type 1 specimen had the average max force of 98 N, displacement at maximum force was 175% and the total elongation of the specimen reached 588 %. One specimen (line colour red) had faster decrease in stress as it fractured faster than the rest. It can be a result of a printing error.

3.2.2. Results of specimen type 2

Specimen type 2 was tested and the results can be seen in table 18 and fig. 50:

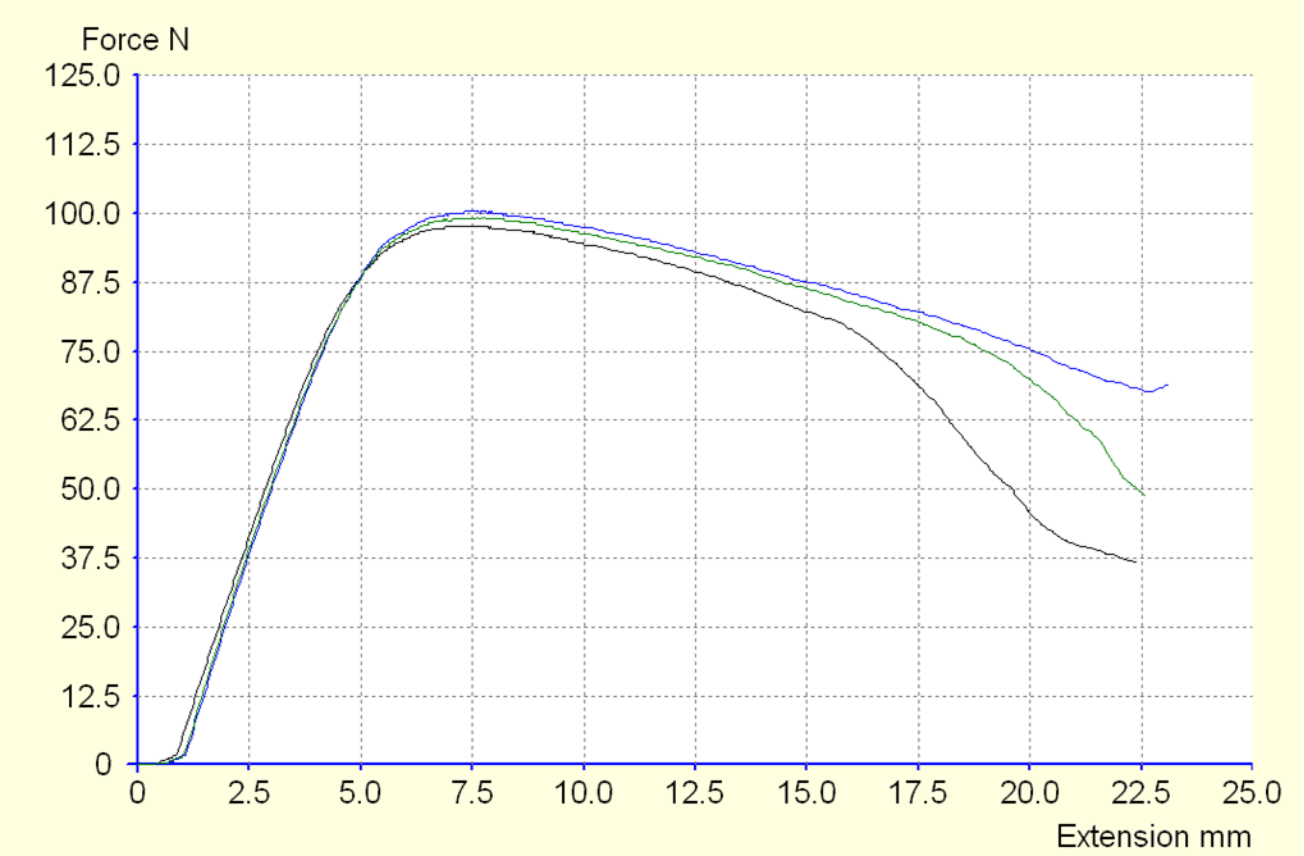

Fig. 50. 3 point bending test results of specimen type 2

Figure 50 depicts the force and displacement relationship of all three type 2 specimens. Maximum values of each specimen can be seen in table 18.

Table 18. Results of specimen type 2

Specimen	Max force, N	Displacement at max, %	Elongation,%
1	97.7	172.5	560
2	100.4	183.1	578
3	99.3	190	565
Mean	99.1	181.9	568
Std. Dev.	1.35	8.82	9.01

The results show that the type 2 specimen had the average max force of 99.1 N, displacement at max force was 181.9 % an the total elongation of the specimen was 568 %. The max force values difference compared to the type 1 is only 1.1%, however the displacement at max stress is 3.9 % bigger that the type 1. One specimen had a similar result as the type 1 where it broke a bit earlier that the rest. This can be caused by the error in printing.

3.2.3. Results of specimen type 3

Specimen type 3 was tested and the results can be seen in table 19 and fig. 51:

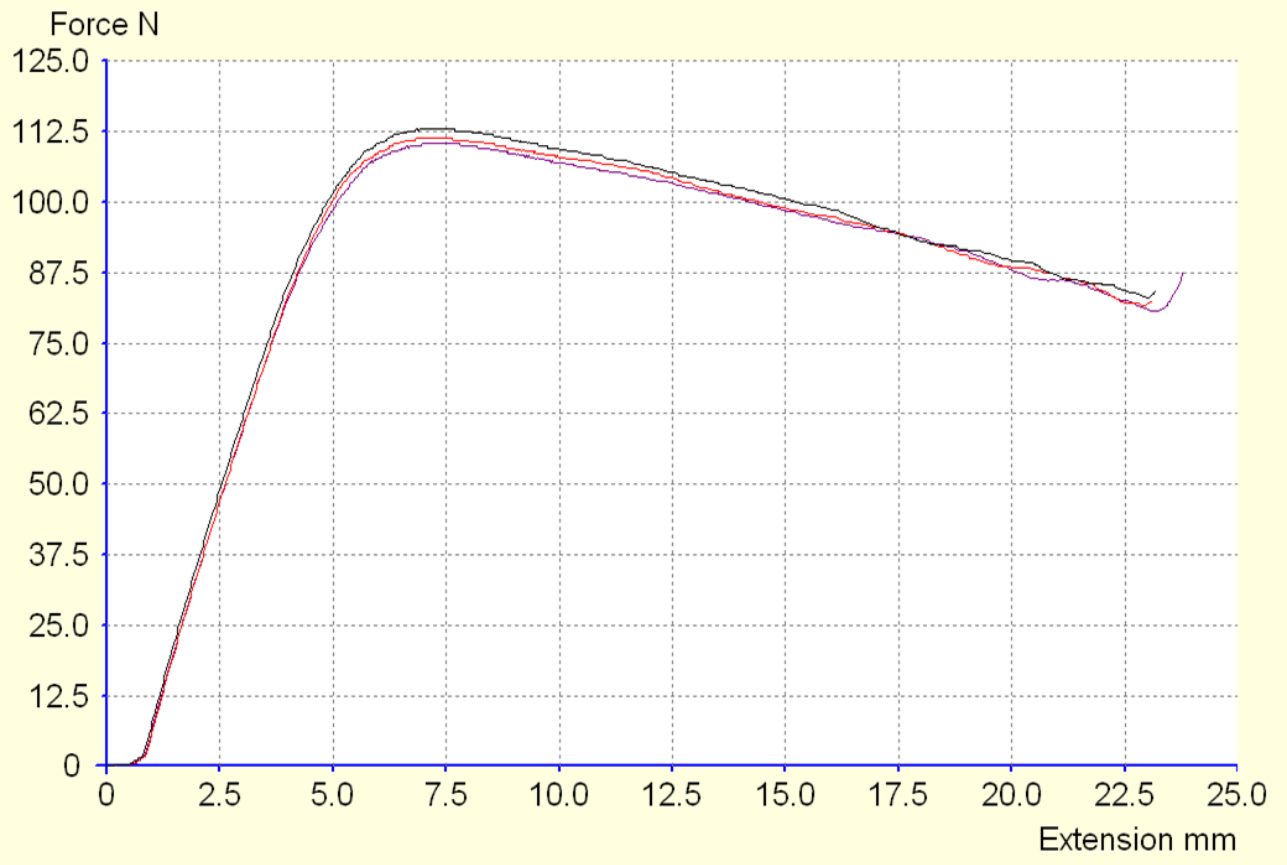

Fig. 51. 3 point bending test results of specimen type 3

Figure 51 depicts the force and displacement relationship of all three type 3 specimens. Maximum values of each specimen can be seen in table 19.

Table 19. Results of specimen type 3

Specimen	Max force, N	Displacement at max, %	Elongation,%
1	110.4	174.4	595
2	111.4	171.3	578
3	113	171.3	580
Mean	111.6	172.3	584
Std. Dev.	1.36	1.80	9.46

The results depicts that the maximum average force of specimens type 3 was 111.6 N, displacement at max force was 172,3 % and the elongation – 584 %. The type 3 had the better results for max force than specimen type 1 and 2 as well as the smallest displacement at max force. All three specimens had very similar graphs, and the testing stopped because the specimens started to touch the supports, hence the curves at the very end of each graph. This shows that the specimens did not brake and had good elasticity throughout all the test.

3.2.4. Results of specimen type 4

Specimen type 4 was tested and the results can be seen in table 20 and fig. 52:

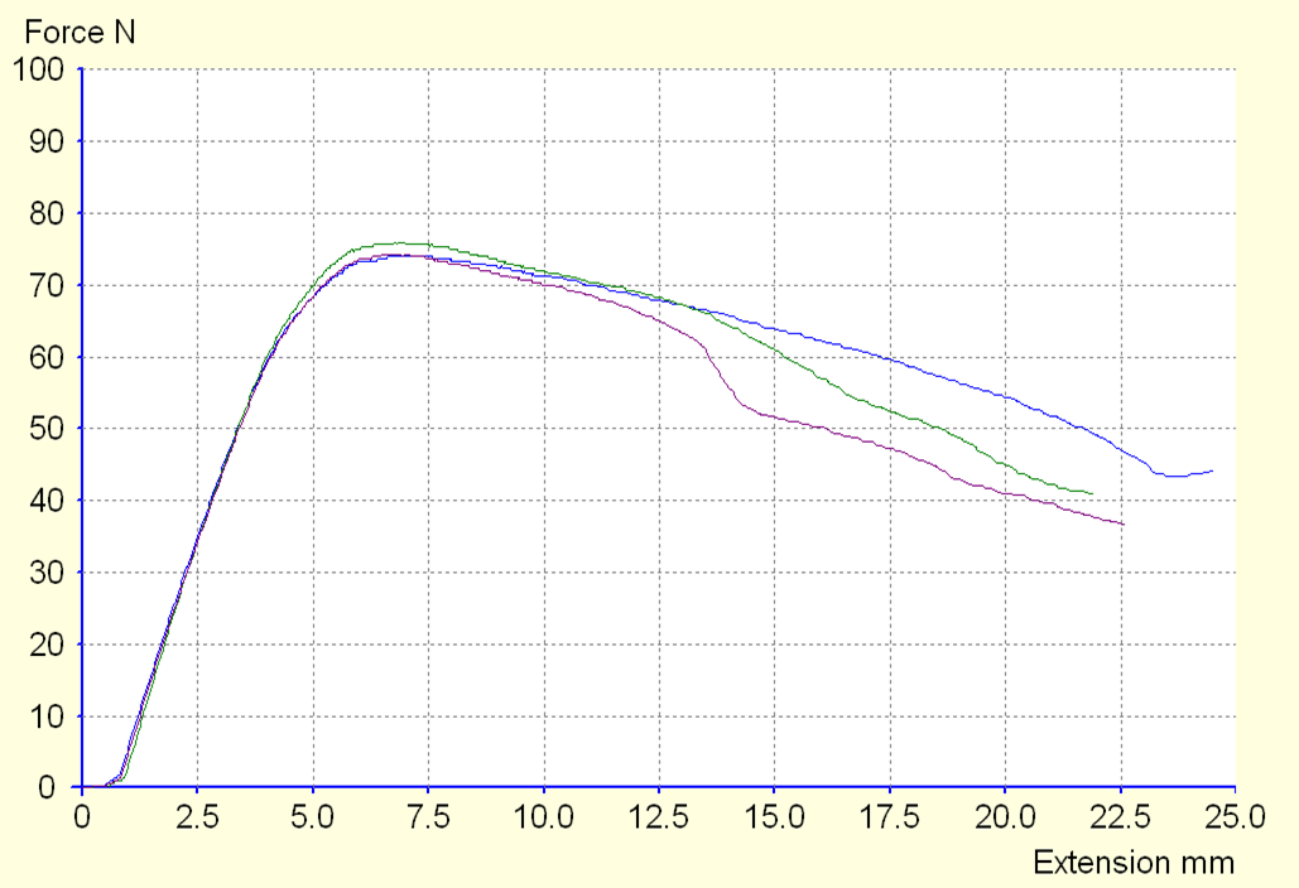

Fig. 52. 3 point bending test results of specimen type 4

Figure 52 depicts the force and displacement relationship of all three type 4 specimens. Maximum values of each specimen can be seen in table 20.

Table 20. Results of specimen type 4

Specimen	Max force, N	Displacement at max, %	Elongation,%
1	74	165.6	613
2	76	168.8	548
3	74.3	161.9	565
Mean	74.8	165.4	575
Std. Dev.	1.10	3.44	33.6

The results show that the maximum average force of specimen type 4 is 74.8 N, displacement at max force is 165.4 %, and the elongation – 575 %. There is a significant decrease in maximum force compared with the first three types as the type 4 has only 60 % infill. One of the specimens had a fracture before the rest and this can be caused by the printing error.

3.2.5. Results of specimen type 5

Specimen type 5 was tested and the results can be seen in table 21 and fig. 53:

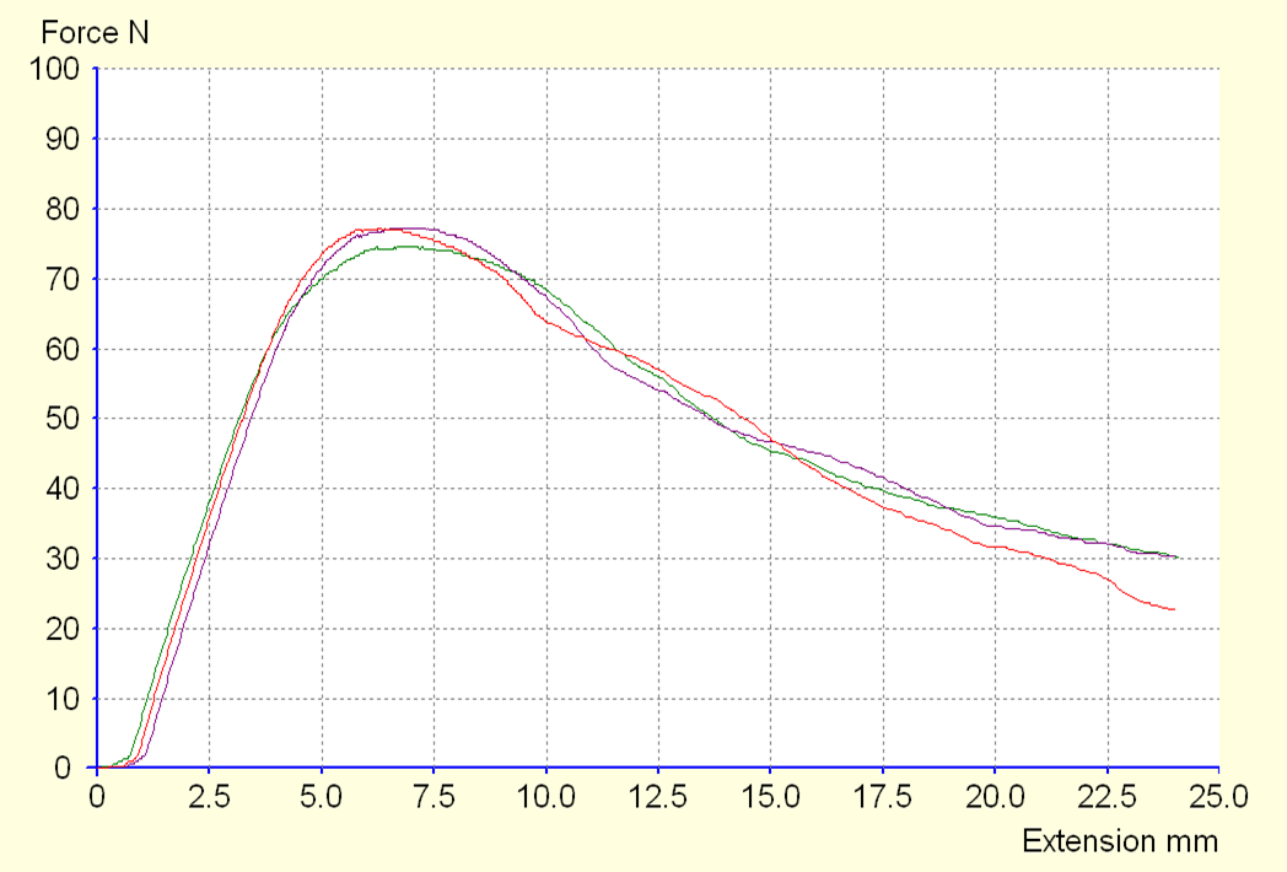

Fig. 53. 3 point bending test results of specimen type 5

Figure 53 depicts the force and displacement relationship of all three type 5 specimens. Maximum values of each specimen can be seen in table 21.

Table 21. Results of specimen type 5

Specimen	Max force, N	Displacement at max, %	Elongation,%
1	74.7	155	603
2	77.3	163.1	600
3	77.3	156.3	600
Mean	76.4	158.1	601
Std. Dev.	1.50	4.38	1.46

The results depicts that the maximum average force of specimens type 3 was 76.4 N, displacement at max force was 158.1 % and the elongation – 601 %. Specimen type 5 has worse max force characteristics that types 1-3 as it has a 60% infill however it has slightly better max force and displacement results that the type 4. Additionally the elongation of the type 5 is the largest. All three specimens had a similar results and small standard deviation.

3.3. Maximum flexural stress calculation and results

In order to determine the flexural properties of the 3D printed specimens and eliminate the geometry aspect, so that the results could be applied to the robot frame construction a flexural stress has to be calculated as follows:

$$\sigma_f = \frac{3FL}{2bd^2}$$

where: σ_f is the flexural stress (Pa); F – applied force (N); L – distance between supports (m); b – the width of test specimen (m), d – thickness of test specimen (m).

The results of flexural stress calculations can be seen in fig. 54:

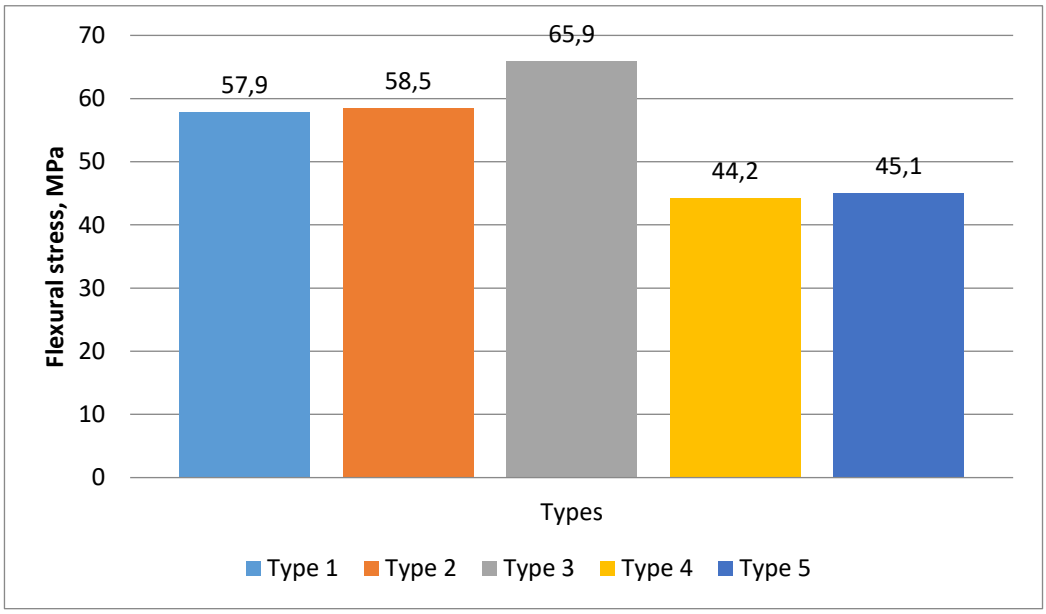

Fig. 54. Flexural stress of different type specimens

The maximum flexural stress that a type 3 specimen could withstand was 65.9 MPa, while the weakest results were shown by the specimen type 4 with only 44.2 MPa.

3.4. Summary

After 3D printing of 5 different types of PLA specimens and performing a 3 point bending test by standard ISO:178, all specimens have shown an elongation of more than 568% each, meaning the printed specimens all have a very good flexural properties. The largest flexural stress – 65.9 MPa was achieved with specimen type 3 (100% infill and concentric infill pattern) while the lowest – 44.2 MPa was achieved with specimen type 4 (60% infill and gyroid infill pattern). Between the first three types that were all 100% infill, a concentric pattern could withstand 13.8% more flexural stress. Meaning the solid infill type has a reasonable impact on the strength of the print. Decreasing the infill by 40% has achieved 32.9% worse results, meaning the decrease in infill is not linear to the decrease in flexural stress and can be used in advantage when the lower flexural stress is required.

4. Social, environmental and economical aspects of wearable assistance rehabilitation robot

The wearable assistance rehabilitation robot plays an important role in person's life and social engagement, is environmental friendly and provides economical benefits as the frame is produced using a 3D printing technology that has numerous advantages over traditional production options.

4.1. Impact on a person's social life

Dysfunction of the upper limb after a stroke can be a devastating experience for the person. A patient not only cannot continue his regular daily life activities as well as stay competitive in a today's job market. This social isolation usually transfers into more serious psychological problems [31-32]. Left alone these problems can evolve into strong forms of depression and other mental illnesses. A person looses interest in all other activities as he/she is feeling as a not fully functioning member of the society. That is why it is extremely important to provide the best possible rehabilitation treatment for the patient in order to bring him/her back to the active everyday life. A regular rehabilitation exercises are mandatory in order to achieve the best results, however regular occupational therapy does not always reach the desired outcome as the quality of the treatment is highly dependent on the qualification of the specialist and the manual excursuses can be usually demotivating and the person quickly looses the interest in them. That is why a wearable assistance rehabilitation robot was designed in order to increase the quality of training and assist not only the patient but the therapist in the rehabilitation cycle. A wearable robot can be helpful to maintain the repeatability of the exercises as well as it can be used not only in the medical institutions as it is wearable and easily transportable. With a resent COVID-19 outbreak, numerous patients were left without the possibility to train as other assistive robots that are already being used cannot be that easily transported and in order for the person to have a regular training sessions one should go to the medicals centre. This possibility was extremely limited during the lockdown. This social isolation problem can be easily solved if a patient would have the wearable robot at home and could continue to exercise with the help of a doctor from a distance using internet communication portals. That is why the designed wearable assistance rehabilitation robot can play a significant role in person's reintegration to the social life and can offer a portable solution if the access to the medical institutions is limited.

4.2. Environmental friendly robot frame

The wearable assistance rehabilitation robot's frame will be 3D printed from PLA plastic. The PLA plastic, unlike other 3D printable plastics is recyclable and biodegradable. Several recycling technologies are listed in fig. 55. Scenario 1 depicts the hydrolysis of PLA waste. At the temperature of 180 degrees and 1.5MPa pressure the PLA is converted to the lactic acid. Scenario 2 depicts the alcoholysis of PLA waste to generate methyl lactate. In this method, chloroform is utilized as a solvent to dissolve the macromolecular PLA, whilst methanol serves as a nucleophile. To produce the product, methyl lactate, the process is carried out at 57 degrees with the aid of stannous octoate as a catalyst. Scenario 3 emphasizes a comprehensive approach to recycling PLA waste by upcycling it for the manufacturing of ethyl lactate. Acetone is used as a more sustainable solvent in this case. As a nucleophile, bio-based ethanol, which may also be obtained from second generation feedstock, is employed. The reaction is carried out at 50 degrees Celsius and at atmospheric pressure in the presence of an organic catalyst to produce ethyl lactate as the result. Scenario 4 is insineration where the PLA plastic waste are used in order to produce

electricity and heat and is widely used as awaste management strategy in most countries emphasysing on circular economy [33-34].

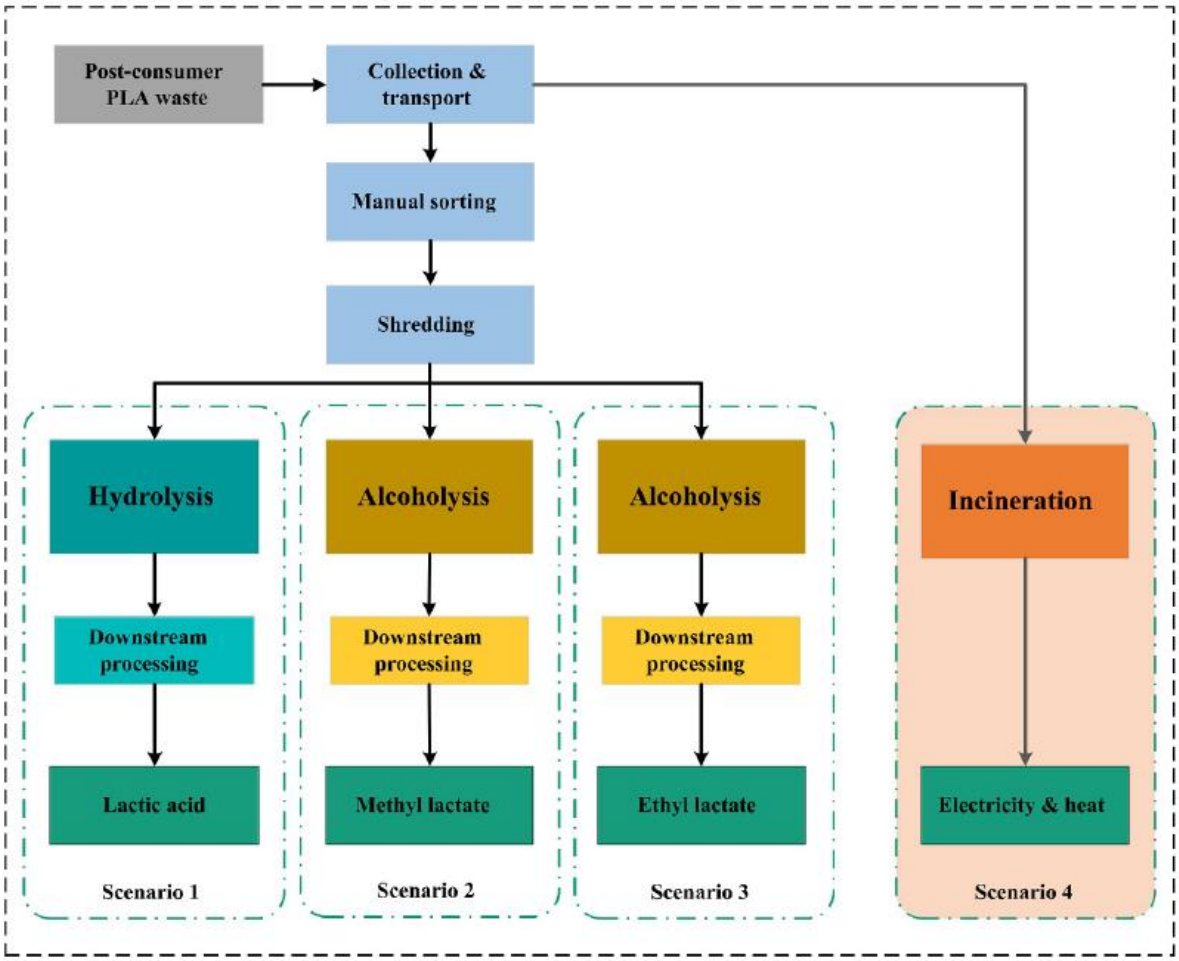

Fig. 55. PLA recycling technologies [33]

PLA is also most commonly studied and used biodegradable plastic under weathering conditions (see fig. 56).

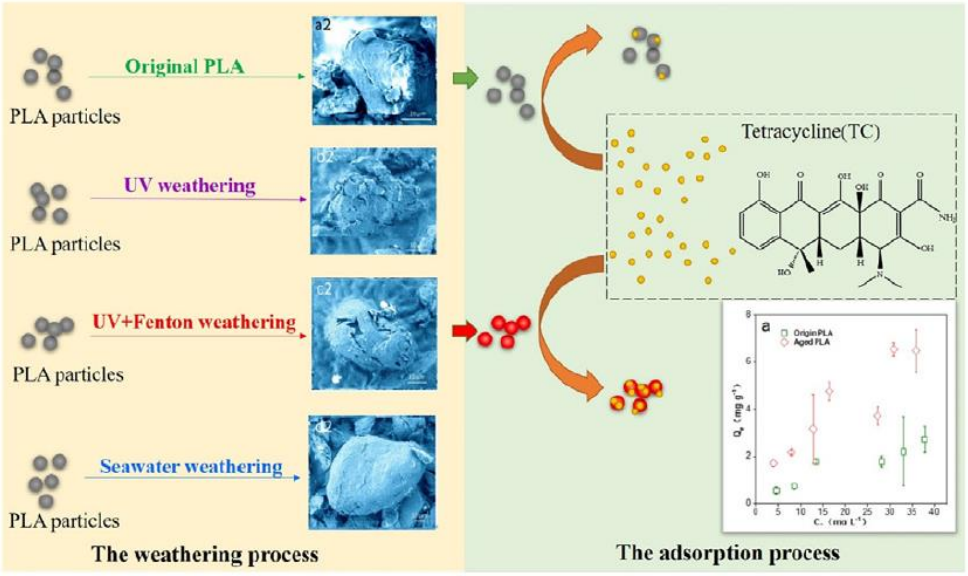

Fig. 56. PLA plastic degradability and absorption under weathering process [35]

PLA may be manufactured directly from natural organic acids or monomer lactic acid molecules as a thermoplastic polymer, and it is quickly destroyed by microbes. Biodegradable plastics, on the other hand, persist in the natural environment as microplastics until they are totally broken down into water and carbon dioxide [35]. The use of PLA plastic as the 3D printing material for the wearable assistance rehabilitation robot's frame will be an eco-friendly solution and will raise awareness for the environmental protection and recycling. The frame from PLA will be 100% recyclable and biodegradable.

4.3. Economical benefits of the selected robot frame production type

The selected production type for the wearable assistance rehabilitation robot's frame is 3D printing. A 3D printing has numerous advantages over the traditional types of production. The time that takes from the idea to the prototype is extremely short for the 3D printing process as the design in CAD systems can be easily transferred to the printer and the prototype can be produced within hours. The price of this experiment is also relatively low in comparison to other production variants as there is no need to make a mold or buy a specific tool for the production. The 3D printer is extremely flexible when it comes to complicated structures as it can use supports to print a difficult in other cases parts. The competitive advantage that a 3D printing process is providing is also important as one can test and launch a new product in a fairly small amount of time and cost. Additionally the quality and consistency aspects are very stable when it comes to 3D printing technology. The tool path is programmed and a margin of error is low. Lastly the sustainability and waste of the 3D printing technology is minimal as almost to none scrap is produced while 3D printing. Milling, turning, molding all have a scrap that has to be machined and removed in order to finish the detail, while the 3D printing prints the detail exactly as it should be without producing any scrap. One exception is the support material scrap as the supports are needed in order to produce complex structures, however the support can be chosen to have minimal infill in this way reducing the waste of material. All these examples prove that there are several economical benefits when choosing the 3D printing technology and the wearable assistance rehabilitation robot frame will be produced with a economically advantageous production process.

4.4. Summary

The designed wearable assistance rehabilitation robot will have a positive impact to the disabled person as it will aid in rehabilitation process, assist in reintegration to the social life and ameliorate ones mental health. The robot frame that is produced from the fully recyclable and biodegradable PLA plastic is ecofriendly and will help to raise the awareness of the environmental pollution. Lastly, the novel 3D printing method has several advantages over the traditional production methods such as availability, testing opportunities, complexity of geometry and low cost.

Discussion

In this paper the wearable assistance rehabilitation robot was developed. The main advantage that distinct this robot from the reviewed analogs is that it can be easily transported and worn at home or desired location. This removes the need to visit the medical institutions every time the exercise is needed and opens up exercising possibilities if the access to these institutions is limited. The further research could implement data of the exercise results recording or online data transfer to the therapist that could analyze them from distance and advise the patient. However this compact design comes with a disadvantage over the competitors as the designed robot is meant for the elbow joint rehabilitation, while the more complex robots are able to exercise more than one joint of the upper limb. The designed robot is at a compromise of flexibility, cost and functionality. The novelty of the design is that a 3D printed robot frame is designed, opening the possibility to use the PLA recyclable and biodegradable plastic. Competitors usually use the other most common construction materials as steel and aluminium, however after the Autodesk Inventor simulations and material research the PLA plastic was selected for this specific designed robot frame as the mechanical properties are satisfactory. In further work robot frame design could be improved – some material could be removed from the parts that do not have to withstand high stresses from FEM simulation results. Regarding the automation side of the robot, the control is carried by the motor controller that can be programmed and receives feedback data from position sensors. The remote controller was designed in order for the person to have a full control over the robot as one will usually use it individually without the supervision of medical personnel. The robot has an implemented lithium ion battery that can last up to 1.5h of exercising. The robot control box was not included in the FEM simulations that could have an impact on the results, meaning further research should be conducted regarding the control box weight impact on the stress calculations, as well as the robot frame and soft padding as a sandwich structure should be analyzed further. An alternative novel control method was also suggested by using a array of tactile sensors in order to control the robot with the wrist movement. The further research should be conducted as the application of this sort is not commonly used, however it can be a promising upgrade for the quality of control aspect of the robot. Lastly a 3 point bending test (standard ISO:178), was conducted in order to determine the flexural properties of the 3D specimen from PLA plastic. Several other researches have been conducted with the 3D printed specimens [36-37]. However the named studies focus on the printing speed, temperature and printing geometry, while the conducted research in this paper combines the dependency of the quantity of infill, geometry of solid infill and the infill pattern geometry allowing to get a better understanding of these parameters and how do they affect the mechanical properties of 3D printed parts. The results show that the best results (65.9 MPa) were achieved with the type 3 specimens as the infill was 100% and the solid infill pattern was concentric. However the types 4 and 5 that had the infill reduced to 60 % showed only 32.9 % worse results (44.2 MPa). This tendency depicts that the decrease in infill does not linearly decrease the flexural stress and that for the wearable assistance rehabilitation robot frame application this feature can be used. As the simulation results were satisfactory and the maximum stress in simulations was selected to be 38 MPa, the type 5 specimen is the closet to being fit (45.1 MPa). Meaning that if the robot frame would be printed with the type 5 parameters the safety factory will be satisfactory and the weight of the frame could be reduced by 40%. The conducted research opened a possibility to save the printing material and lessen the weight of the robot frame. A further research could be conducted with more specimen sample size in the future in order to optimize the printing process and further reduce the weight of the robot frame.

Conclusions

1. After analyzing the different types of exoskeletons and control methods, a wearable exoskeleton type with a control method based on feedback sensor data and position control was selected in order to develop lightweight and portable wearable assistance rehabilitation robot with a user friendly and reliable control method.
2. The frame for the wearable assistance rehabilitation robot was designed and after the material research was conducted PLA plastic was selected as the main material and 3D printing FDM technology was selected for the production of the frame. Stress analysis were performed using the Autodesk Inventor software, where the highest Von Misses stress was 11.27 MPa, as well as the highest displacement 2.22 mm on the forearm frame part. The minimum safety factor was 3.37 being satisfactory. The frame was designed to withstand the required stress and lightweight, weighting 0.68 kg.
3. In order to ensure proper control of the wearable assistance rehabilitation robot the motor-gearbox was selected for the rated torque of 5.2 Nm. A motor controller was implemented that enables torque, speed and brake control. Two inductive proximity sensors were selected for the position feedback and a kill switch bracelet was chosen to ensure the safety of the wearer. A control algorithm based on the remote controller input was developed for user friendly control.
4. A research was conducted using five different types of 3D printed specimens from PLA plastic and performing a 3 point bending test using ISO:178 standard. The specimens varied in infill, solid infill paters and infill geometry patterns. The best results of flexural stress were achieved using a solid infill and concentric geometry pattern – 65.9 MPa, while the worst results were by using a 60% infill and gyroid infill geometry – 44.2 MPa. All specimens have shown an elongation of more than 568% each, meaning the printed specimens had good flexural properties.
5. The designed wearable assistance rehabilitation robot will aid in minimising the social isolation of the disabled person and help to reintegrate one to the society. The frame of the robot is designed from the PLA material that is environmental friendly, being fully recyclable and biodegradable, while the selected 3D printing production method has several economical benefits such as production speed, testing possibilities and low expenses compared to traditional production methods.

List of References

1. Bowen Xiao, Lin Chen, Xin Zhang, Zengyong Li, Xiaoyu Liu, Xiaoying Wu, Wensheng Hou. Design of a virtual reality rehabilitation system for upper limbs that inhibits compensatory movement, Medicine in Novel Technology and Devices, Volume 13, 2022, 100110, ISSN 2590-0935. [watched: 2023 02 11]. Access via: https://www.sciencedirect.com/science/article/pii/S2590093521000540
2. QINGCONG WU, YING CHEN. Variable admittance time-delay control of an upper limb rehabilitation robot based on human stiffness estimation, Mechatronics, Volume 90, 2023, 102935, ISSN 0957-4158. [watched: 2023 02 11]. Access via: https://www.sciencedirect.com/science/article/pii/S0957415822001532
3. WENXI LI, DONGSHENG XU. Application of intelligent rehabilitation equipment in occupational therapy for enhancing upper limb function of patients in the whole phase of stroke, Medicine in Novel Technology and Devices, Volume 12, 2021, 100097, ISSN 2590-0935. [watched: 2023 02 11]. Access via: https://www.sciencedirect.com/science/article/pii/S2590093521000412
4. Hui Liang, Shiqing Liu, Yi Wang, Junjun Pan, Yazhou Zhang, Xiaohang Dong. Multi-user upper limb rehabilitation training system integrating social interaction, Computers & Graphics, Volume 111, 2023, Pages 103-110, ISSN 0097-8493. [watched: 2023 02 11]. Access via: https://www.sciencedirect.com/science/article/pii/S0097849323000079
5. JIANFENG LI, QIANG CAO, CHUNZHAO ZHANG, CHUNJING TAO, RUN JI. Position solution of a novel four-DOFs self-aligning exoskeleton mechanism for upper limb rehabilitation, Mechanism and Machine Theory, Volume 141, 2019, Pages 14-39, ISSN 0094-114X. [watched: 2023 02 12]. Access via: https://www.sciencedirect.com/science/article/pii/S0094114X1832216X
6. ERKAN ÖDEMIŞ, CABBAR VEYSEL BAYSAL. Development of a participation assessment system based on multimodal evaluation of user responses for upper limb rehabilitation, Biomedical Signal Processing and Control, Volume 70, 2021, 103066, ISSN 1746-8094. [watched: 2023 02 12]. Access via: https://www.sciencedirect.com/science/article/pii/S1746809421006637
7. JING BAI, AIGUO SONG, TING WANG, HUIJUN LI. A novel backstepping adaptive impedance control for an upper limb rehabilitation robot, Computers & Electrical Engineering, Volume 80, 2019, 106465, ISSN 0045-7906. [watched: 2023 02 12]. Access via: https://www.sciencedirect.com/science/article/pii/S0045790619305324
8. S. DEHEM, M. GILLIAUX, G. STOQUART, C. DETREMBLEUR, T. LEJEUNE. Effectiveness of upper limb robotic-assisted therapy in the early phase of stroke rehabilitation: A single-blind, randomised, controlled trial, Annals of Physical and Rehabilitation Medicine, Volume 61, Supplement, 2018, Page e25, ISSN 1877-0657. [watched: 2023 02 12]. Access via: https://www.sciencedirect.com/science/article/pii/S1877065718301283
9. LEE, S.H., PARK, G., CHO, D.Y. *ET AL*. Comparisons between end-effector and exoskeleton rehabilitation robots regarding upper extremity function among chronic stroke patients with moderate-to-severe upper limb impairment. *Sci Rep* 10, 1806, 2020. [watched: 2023 02 17]. Access via: https://www.nature.com/articles/s41598-020-58630-2#citeas

10. LAZAREVIĆ, MIHAILO & ŽIVKOVIĆ, NIKOLA & RADOJEVIĆ, DARKO. Open-closed Iterative Learning Control Algorithm for Exoskeleton Rehabilitation Purposes. 2019. MATEC Web of Conferences. 292. 01010. 10.1051/matecconf/201929201010. [watched: 2023 02 17]. Access via: https://www.researchgate.net/publication/336009634_Open-closed_Iterative_Learning_Control_Algorithm_for_Exoskeleton_Rehabilitation_Purposes
11. ZHANG, L.; GUO, S.; SUN, Q. Development and Assist-As-Needed Control of an End-Effector Upper Limb Rehabilitation Robot. Appl. Sci. 2020, *10*, 6684. [watched: 2023 02 17]. Access via: https://www.mdpi.com/2076-3417/10/19/6684
12. PANG, ZAIXIANG & WANG, TONGYU & YU, JUNZHI & WANG, ZHANLI & LIU, SHUAI & ZHANG, XIYU. Design and analysis of shoulder joint exoskeleton rehabilitation mechanism based on gear and rack transmission. 2021. AIP Advances. 11. 055122. 10.1063/5.0051484. [watched: 2023 02 17]. Access via: https://www.researchgate.net/publication/351640611_Design_and_analysis_of_shoulder_joint_exoskeleton_rehabilitation_mechanism_based_on_gear_and_rack_transmission
13. Zhongyi Li, Weihai Chen, Jianbin Zhang, Qihang Li, Jianhua Wang, Zaojun Fang, Guilin Yang. A novel cable-driven antagonistic joint designed with variable stiffness mechanisms, Mechanism and Machine Theory, Volume 171, 2022, 104716, ISSN 0094-114X. [watched: 2023 02 17]. Access via: https://www.sciencedirect.com/science/article/pii/S0094114X21004432
14. YIDA GUO, HAOPING WANG, YANG TIAN, DARWIN G. CALDWELL. Task performance-based adaptive velocity assist-as-needed control for an upper limb exoskeleton, Biomedical Signal Processing and Control, Volume 73, 2022, 103474, ISSN 1746-8094. [watched: 2023 02 18]. Access via: https://www.sciencedirect.com/science/article/abs/pii/S1746809421010715
15. PAWEŁ HERBIN, MIROSŁAW PAJOR. Human-robot cooperative control system based on serial elastic actuator bowden cable drive in ExoArm 7-DOF upper extremity exoskeleton, Mechanism and Machine Theory, Volume 163, 2021, 104372, ISSN 0094-114X. [watched: 2023 02 18]. Access via: https://www.sciencedirect.com/science/article/pii/S0094114X21001300
16. JIANFENG LI, QIANG CAO, MINGJIE DONG, CHUNZHAO ZHANG. Compatibility evaluation of a 4-DOF ergonomic exoskeleton for upper limb rehabilitation, Mechanism and Machine Theory, Volume 156, 2021, 104146, ISSN 0094-114X. [watched: 2023 02 18]. Access via: https://www.sciencedirect.com/science/article/pii/S0094114X20303633
17. ZANCHETTIN, ANDREA MARIA & ROCCO, PAOLO & BASCETTA, LUCA & SYMEONIDIS, IOANNIS & PELDSCHUS, STEFFEN. Kinematic motion analysis of the human arm during a manipulation task. Joint 41st International Symposium on Robotics and 6th German Conference on Robotics 2010, ISR/ROBOTIK 2010. 2. 1-6. [watched: 2023 02 18]. Access via: https://www.researchgate.net/publication/261021019_Kinematic_motion_analysis_of_the_human_arm_during_a_manipulation_task

18. RAMACHANDRAN, HARI & VASUDEVAN, DEVANANDH & BRAHMA, ADITYA & PUGAZHENTHI, S.. Estimation of mass moment of inertia of human body, when bending forward, for the design of a self-transfer robotic facility. Journal of Engineering Science and Technology. 2016. 11. 166-176. [watched: 2023 02 20]. Access via: https://www.researchgate.net/publication/271292606_Estimation_of_mass_moment_of_inertia_of_human_body_when_bending_forward_for_the_design_of_a_self-transfer_robotic_facility
19. RAVIKUMAR PATEL, CHIRAG DESAI, SAGARSINGH KUSHWAH, M.H. MANGROLA. A review article on FDM process parameters in 3D printing for composite materials, Materials Today: Proceedings, Volume 60, Part 3, 2022, Pages 2162-2166, ISSN 2214-7853. [watched: 2023 04 01]. Access via: https://www.sciencedirect.com/science/article/pii/S2214785322010252
20. N. LOKESH, B.A. PRAVEENA, J. SUDHEER REDDY, VIKRAM KEDAMBADI VASU, S. VIJAYKUMAR. Evaluation on effect of printing process parameter through Taguchi approach on mechanical properties of 3D printed PLA specimens using FDM at constant printing temperature, Materials Today: Proceedings, Volume 52, Part 3, 2022, Pages 1288-1293, ISSN 2214-7853. [watched: 2023 04 01]. Access via: https://www.sciencedirect.com/science/article/pii/S2214785321070607
21. TAMIR, T.S., XIONG, G., FANG, Q. A feedback-based print quality improving strategy for FDM 3D printing: an optimal design approach. Int J Adv Manuf Technol 120, 2777–2791, 2022. [watched: 2023 04 01]. Access via: https://link.springer.com/article/10.1007/s00170-021-08332-4
22. Pete Millett. Brushless vs. Brushed DC Motors: When and Why to Choose One Over the Other. MPS. 2022. [watched: 2023 04 01]. Access via: https://www.monolithicpower.com/en/brushless-vs-brushed-dc-motors
23. NANOTEC. Brushless DC motors and gearboxes [online]. [watched: 2023 04 01]. Access via: https://en.nanotec.com/
24. AUTOMATION DIRECT. Inductive proximity sensor Contridex DW-AD-711-04 [online]. [watched: 2023 04 02]. Access via: https://www.automationdirect.com/adc/shopping/catalog/sensors_-z-_encoders/inductive_proximity_sensors/4mm_round/dw-ad-711-04
25. AMAZON. Kill switch wrist strap [online]. [watched: 2023 04 02]. Access via: https://www.amazon.com/CAMNWAMN-Replacement-EW2-68348-00-00-WaveVenture-WaveBlaster/dp/B099WR2KVZ
26. NANOTEC. Motor controller C5-E-2-09 [online]. [watched: 2023 04 08]. Access via: https://en.nanotec.com/products/1768-c5-e-2-09-motor-controller-drive-for-canopen-or-usb
27. DNK. 24V 3Ah Lithium ion Battery Pack, DNK-LTB2430 [online]. [watched: 2023 04 22]. Access via: https://www.dnkpower.com/products/24v-3ah-lithium-ion-battery-pack
28. BYUN, S.-W & LEE, S.-P. Hand gesture recognition suitable for wearable devices using flexible epidermal tactile sensor array. 2018. Journal of Electrical Engineering and Technology. 13. 1731-1738. 10.5370/JEET.2018.13.4.1731. [watched: 2023 05 01]. Access via: https://www.researchgate.net/publication/326127745_Hand_gesture_recognition_suitable_for_wearable_devices_using_flexible_epidermal_tactile_sensor_array

29. CREALITY. Creality HP PLA 3D Printer Filaments [online]. [watched: 2023 05 06]. Access via: https://www.creality3dofficial.eu/products/2kg-creality-hp-pla-3d-printer-filaments
30. KTU APCIS. Tinius Olsen H10KT [online]. [watched: 2023 05 06]. Access via: https://apcis.ktu.edu/lt/site/katalogas?more=8870
31. MARIEKE M. VISSER, MAJANKA H. HEIJENBROK-KAL, ADRIAAN VAN'T SPIJKER, KRISTINE M. OOSTRA, JAN J. BUSSCHBACH, GERARD M. RIBBERS. Coping, Problem Solving, Depression, and Health-Related Quality of Life in Patients Receiving Outpatient Stroke Rehabilitation. Archives of Physical Medicine and Rehabilitation, Volume 96, Issue 8, 2015, Pages 1492-1498, ISSN 0003-9993. [watched: 2023 05 06]. Access via: https://www.sciencedirect.com/science/article/abs/pii/S0003999315003731
32. BIBO YANG, YANHUAN HUANG, ZENGYONG LI, XIAOLING HU. Management of post-stroke depression (PSD) by electroencephalography for effective rehabilitation. Engineered Regeneration, Volume 4, Issue 1, 2023, Pages 44-54, ISSN 2666-1381. [watched: 2023 05 07]. Access via: https://www.sciencedirect.com/science/article/pii/S266613812200072X
33. VENKAT ARYAN, DANIEL MAGA, PRANAV MAJGAONKAR, RONNY HANICH. Valorisation of polylactic acid (PLA) waste: A comparative life cycle assessment of various solvent-based chemical recycling technologies, Resources, Conservation and Recycling, Volume 172, 2021, 105670, ISSN 0921-3449. [watched: 2023 05 07]. Access via: https://www.sciencedirect.com/science/article/pii/S0921344921002792
34. PRANAV MAJGAONKAR, RONNY HANICH, FRANK MALZ, ROBERT BRÜLL. Chemical Recycling of Post-Consumer PLA Waste for Sustainable Production of Ethyl Lactate, Chemical Engineering Journal, Volume 423, 2021, 129952, ISSN 1385-8947. [watched: 2023 05 07]. Access via: https://www.sciencedirect.com/science/article/pii/S1385894721015369
35. QIYU QIN, YIDI YANG, CHANGFU YANG, LEILIHE ZHANG, HAOYUAN YIN, FEI YU, JIE MA. Degradation and adsorption behavior of biodegradable plastic PLA under conventional weathering conditions. Science of The Total Environment, Volume 842, 2022, 156775, ISSN 0048-9697. [watched: 2023 05 07]. Access via: https://www.sciencedirect.com/science/article/pii/S0048969722038724
36. GURCAN ATAKOK, MENDERES KAM, HANIFE BUKRE KOC. Tensile, three-point bending and impact strength of 3D printed parts using PLA and recycled PLA filaments: A statistical investigation, Journal of Materials Research and Technology, Volume 18, 2022, Pages 1542-1554, ISSN 2238-7854. [watched: 2023 05 07]. Access via: https://www.sciencedirect.com/science/article/pii/S2238785422003192
37. OTHMAN, MOHD SARHAN & MISRAN, MOHD & ZA'ABA, HELMI. Study on Mechanical Properties of Pla Printed using 3D Printer. 2019. [watched: 2023 05 07]. Access via: https://www.researchgate.net/publication/346713811_Study_on_Mechanical_Properties_of_Pla_Printed_using_3D_Printer

Appendices

Appendix 1. Technical data of the brushless DC motor DFA68M024037-A.

TECHNICAL DATA

Rated Current	5.6 A	Line to Line Resistance	0.25 Ohm
Line to Line Inductance	0.2 mH	Rotor Inertia	1000 gcm²
Torque Constant	5.4 Ncm/A	Weight	0.47 kg
Motor Connection	Open Cable End	Peak Current	17 A
Peak Torque	87 Ncm	Length "A"	42 mm
Rated Power	110 W	Rated Torque	29 Ncm
Rated Speed	3700 rpm	Rated Voltage	24 V
Size	68 mm		

Appendix 2. Technical data of the planetary gearbox GP56-S2-20-SR.

TECHNICAL DATA

For Motor Size	68 mm (BLDC), NEMA 23, NEMA 24	Type	Standard Bearing
Efficiency	89 %	Max. Backlash	32 ´(arc minutes)
Rated Output Torque	28.6 Nm	Max. Output Torque	39.4 Nm
Reduction Ratio	20.03	Max. Input Speed	8304 rpm
Moment of Inertia	3.4 kg mm²	Service Life	10000 h
Operating Temperature	-15 °C - 90 °C	Length "L"	61.8 mm
Flange Length L1	6 mm	Weight	0.79 kg
Admissible Axial Shaft Load	1302 N	Admissible Radial Shaft Load	516 N
IP-Protection Gearbox	IP54		

Appendix 3. Technical data of the 3D printer Creality CR-10S

CR 10S parameter

Machine color	Orange、 blue、 black(optional)
Forming technology	FDM
Print size	300×300×400mm
Machine net weight	9kg
Packing weight	13.8Kg
Nozzle Diameter	Standard 0.4mm
Control system	Win、 xp、 mac、 vista、 Linux
Software	Cura、 Simplify3D、 Repetier-host
File format	STL、 OBJ、G-Code
Print speed	Normal 60mm/s. Max 100mm/s
Filament diameter	1.75mm
Support filament	PL/ABS/TPU/wood/carbon fiber/Copper
Power requirement	Input:110V-220V, Output 12V, Power 270W

Appendix 4. Assemble of wearable assistance rehabilitation robot

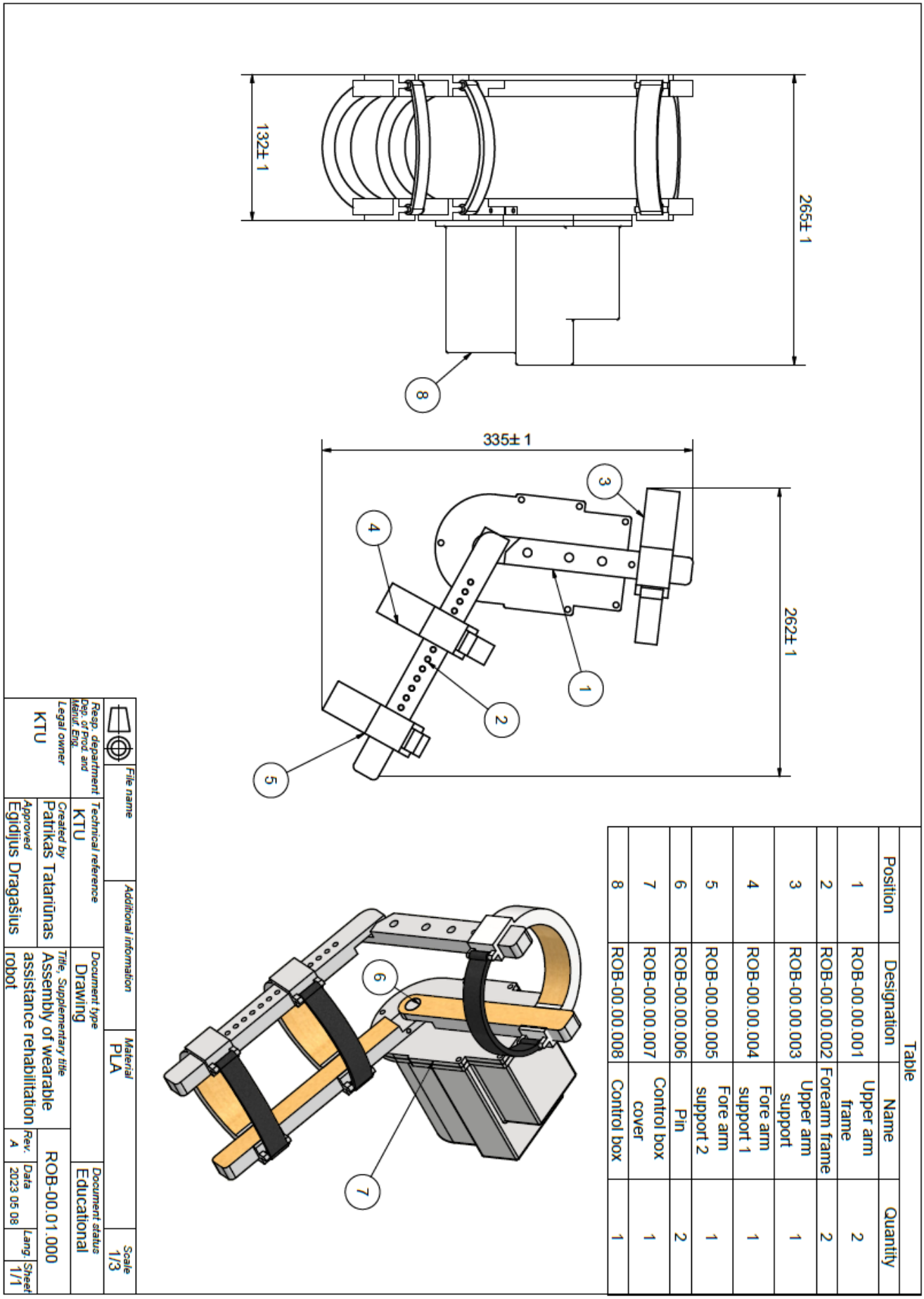

Table

Position	Designation	Name	Quantity
1	ROB-00.00.001	Upper arm frame	2
2	ROB-00.00.002	Forearm frame	2
3	ROB-00.00.003	Upper arm support	1
4	ROB-00.00.004	Fore arm support 1	1
5	ROB-00.00.005	Fore arm support 2	1
6	ROB-00.00.006	Pin	2
7	ROB-00.00.007	Control box cover	1
8	ROB-00.00.008	Control box	1

Resp. department Dep. of Prod. and Manuf. Eng.	File name	Additional information	Material PLA		Scale 1/3
Legal owner KTU	Technical reference KTU		Document type Drawing		Document status Educational
Created by Patrikas Tatariūnas	Title, Supplementary title Assembly of wearable assistance rehabilitation robot			Rev. A	ROB-00.01.000
Approved Egidijus Dragašius				Data 2023 05 08	Lang. Sheet 1/1